

AD



TECHNICAL REPORT ECOM 02032-3

AD 653638

RESEARCH ON
DISTRIBUTED FERRITES
FOR
CROSSED-FIELD MICROWAVE DEVICES

QUARTERLY REPORT

by

W.A. Smith - D. Masse - J.M. Osepchuk

R. Plumridge - L. Tisdale

MAY 1967

.....
ECOM

UNITED STATES ARMY ELECTRONICS COMMAND - FORT MONMOUTH, N.J.

Sponsored by: ADVANCED RESEARCH PROJECTS AGENCY - PROJECT DEFENDER
ARPA Order No. 679, Amendment No. 1

Contract No.: DA28-043-AMC-02032(E)

DISTRIBUTION STATEMENT

DISTRIBUTION OF THIS
DOCUMENT IS UNLIMITED

RAYTHEON COMPANY
MICROWAVE AND POWER TUBE DIVISION
Waltham, Massachusetts

ARCHIVE COPY

Technical Report ECOM 02032-3

January 1967

RESEARCH ON DISTRIBUTED FERRITES
FOR
CROSSED-FIELD MICROWAVE DEVICES

3rd Quarterly Report

10 August - 9 November 1966

Report No. 3

Contract No. DA28-043-AMC-02032(E)

Prepared by

W. A. Smith - D. Masse - J. M. Osepchuk - R. Plumridge - L. Tisdale

RAYTHEON COMPANY
Microwave and Power Tube Division
Waltham, Massachusetts

For

U. S. Army Electronics Command
Fort Monmouth, N. J. 07703

Sponsored by

Advanced Research Projects Agency
ARPA Order No. 679
Amendment No. 1

DISTRIBUTION STATEMENT

Distribution of This Document is Unlimited



NOTICES

Disclaimers

The findings in this report are not to be construed as an official Department of the Army position, unless so designated by other authorized documents.

The citation of trade names and names of manufacturers in this report is not to be construed as official Government indorsement or approval of commercial products or services referenced herein.

Disposition

Destroy this report when it is no longer needed.
Do not return it to the originator.

ABSTRACT

The objective of this program is to develop the knowledge and technology necessary to take full advantage of the unidirectional attenuative properties of ferrites in achieving improved gain and bandwidth in crossed-field microwave amplifiers and oscillators. During the third quarterly period, activities included cold testing of ferrite materials in conjunction with an L-band helix and an investigation of narrow linewidth ferrites in an S-band Amplitron.

Theoretical and experimental studies indicated that broadbanding of ferrites in a CFA can be accomplished by broader linewidths, porous ferrites, or by a combination of both methods. Measurements made on a porous magnesium ferrite support this conclusion.

Bonding of ferrites to dielectric can be effected by the use of glass frit, and bonding to copper can be accomplished by sputtering nickel onto the ferrite in an argon atmosphere and subsequently brazing with silfos solder.

TABLE OF CONTENTS

<u>Section</u>		<u>Page</u>
1.	Purpose	1
2.	Scope	1
3.	The Cold Test Program	2
	3.1 Cold Test Results	5
	3.2 Cold Tests - Ferrites in the Amplitron	15
4.	Survey of Ferrite Materials	19
	4.1 Evaluation of Material #40 from Sperry Micro-wave Co.	19
	4.2 Broadening Techniques	25
	4.2.1 Using a Broad Linewidth Material	28
	4.2.2 Using a Staggered Construction	28
	4.2.3 Using Porous Ferrite	30
	4.3 Use of Narrow Linewidth Material	30
5.	Ferrite Materials Research	31
6.	Ferrite Bonding	33
	6.1 Ferrite - Ceramic Bonds	33
	6.1.1 Mechanical Strength	33
	6.1.2 Magnetic Properties	33
	6.1.3 Thermal Conductivity	33
	6.2 Ferrite to Metal Bonds	34
	6.2.1 Preparation of Metallized Film	34
7.	Conclusion	34

LIST OF ILLUSTRATIONS

<u>Figure</u>		<u>Page</u>
3-1	Helix Delay Line Cross-Sectional View	3
3-2	QKS1267 Delay Line Assembly (with Ferrite Ring)	4
3-3	Percent Voltage Reflection between Coaxial Input and Helix Line	6
3-4	Impedance Match - Helix - Coaxial Inputs	6
3-5	Helix - Backward Wave Power Loss (db)	6
3-6	Helix - Forward Wave Power Loss (db)	7
3-7	Helix - Backward Wave Power Loss (db)	7
3-8	Helix - Forward Wave Power Loss (db)	7
3-9	Helix - Backwave Wave Power Loss (db)	9
3-10	Helix - Backward Wave Power Loss (db)	9
3-11	Helix - Backward Wave Power Loss (db)	10
3-12	Helix - Forward Wave Loss (db)	10
3-13	Helix - Backward Wave Power Loss (db)	11
3-14	Helix - Backward Wave Power Loss (db)	11
3-15	Dielectric Box and Ferrite for Helix Delay Line (12" long)	12
3-16	Helix - Backward Wave Power Loss	12
3-17	Helix - Forward Wave Power Loss	13
3-18		13
3-19	Percent Voltage Transmission Port 2 to 4	14
3-20	Helix - Percent Voltage Transmission from Port 1 to 4	14
4-1	Resonance Condition $b/a = f(4\pi Ms, Ha)$ for $\omega_r = 6000 \text{ MHz}$, $\gamma = 2.8$	20
4-2	Resonance Condition $b/a = f(4\pi Ms, Ha)$ for $\omega_r = 1500 \text{ MHz}$, $\gamma = 3.55$	21
4-3	Resonance Condition $b/a = f(4\pi Ms, Ha)$ for $\omega_r = 3000 \text{ MHz}$, $\gamma = 3.55$	22
4-4	Resonance Condition $b/a = f(4\pi Ms, Ha)$ for $\omega_r = 6000 \text{ MHz}$, $\gamma = 3.55$	23
4-5	Resonance Condition $b/a = f(4\pi Ms, Ha)$ for $\omega_r = 10,000 \text{ MHz}$, $\gamma = 3.55$	24
4-6	Sperry Microwave Electronics Co. Material #40 $4\pi Ms$ vs Temperature	26
4-7	Sperry Microwave Electronics Material #40 $\mu"$ vs Applied Magnetic Field (Measured at S-Band)	27
5-1	Measurement Data for Linewidth of Magnesium Ferrite at X-Band	32
5-2	Linewidth of Polycrystalline YIG vs Temperature	32

BLANK PAGE

1. PURPOSE

The objective of this program is to develop the knowledge and technology needed to take full advantage of the unidirectional attenuative properties of ferrites in achieving improved gain and bandwidth in crossed-field microwave amplifiers and oscillators. This objective will be achieved by reducing circuit feedback and reflections with minimum insertion loss through the use of ferromagnetic materials. Improvement of compactness and weight will also result from utilization of ferromagnetic materials in crossed-field devices.

2. SCOPE

The program consists of a theoretical and experimental study of various problem areas. The emphasis in this program will be on the interaction of ferrites with broadband delay lines suitable for crossed-field devices. The experimental work may be conducted at any convenient microwave frequency. However, both the experimental and the theoretical information must be such that it can be utilized at all microwave frequencies up to 10 GHz. The particular tasks to be undertaken will be as outlined in U. S. Army Electronics Command Guideline No. MW-47, dated 2 September 1965.

3. THE COLD TEST PROGRAM

Cold test activities during this report period included further study of distributed ferrites in conjunction with an L-band helix, and an investigation of narrow linewidth ferrites to damp a band-edge oscillation problem in an S-band Amplitron.

The helix geometry was as indicated by Figure 3-1. Ferrite was introduced in the form of long slabs (12 inches in the direction of propagation) centered between the 50 ohm input and output rf connectors. For the L-band tests, a Raytheon nickel-aluminum ferrite, #R-142, was used. This material has a $4\pi Ms$ value of 450 gauss and a line width, ΔH , in the vicinity of 300 oersteds. As shown by Figure 3-1, the ferrite material was located between the flattened helix and the backwall.

For a slab of cross-section $l = 0.400$ inch and thickness $\Delta x = 0.090$ inch, the computed value of resonance field at 1.5 GHz is 460 oersteds. The demagnetization factors used in the computation were

$$N_x = \frac{l}{l + \Delta x} \quad N_z = 0 \quad N_y = \frac{\Delta x}{l + \Delta x} \quad (3-1)$$

Backward-wave attenuation was computed by means of the following expression.

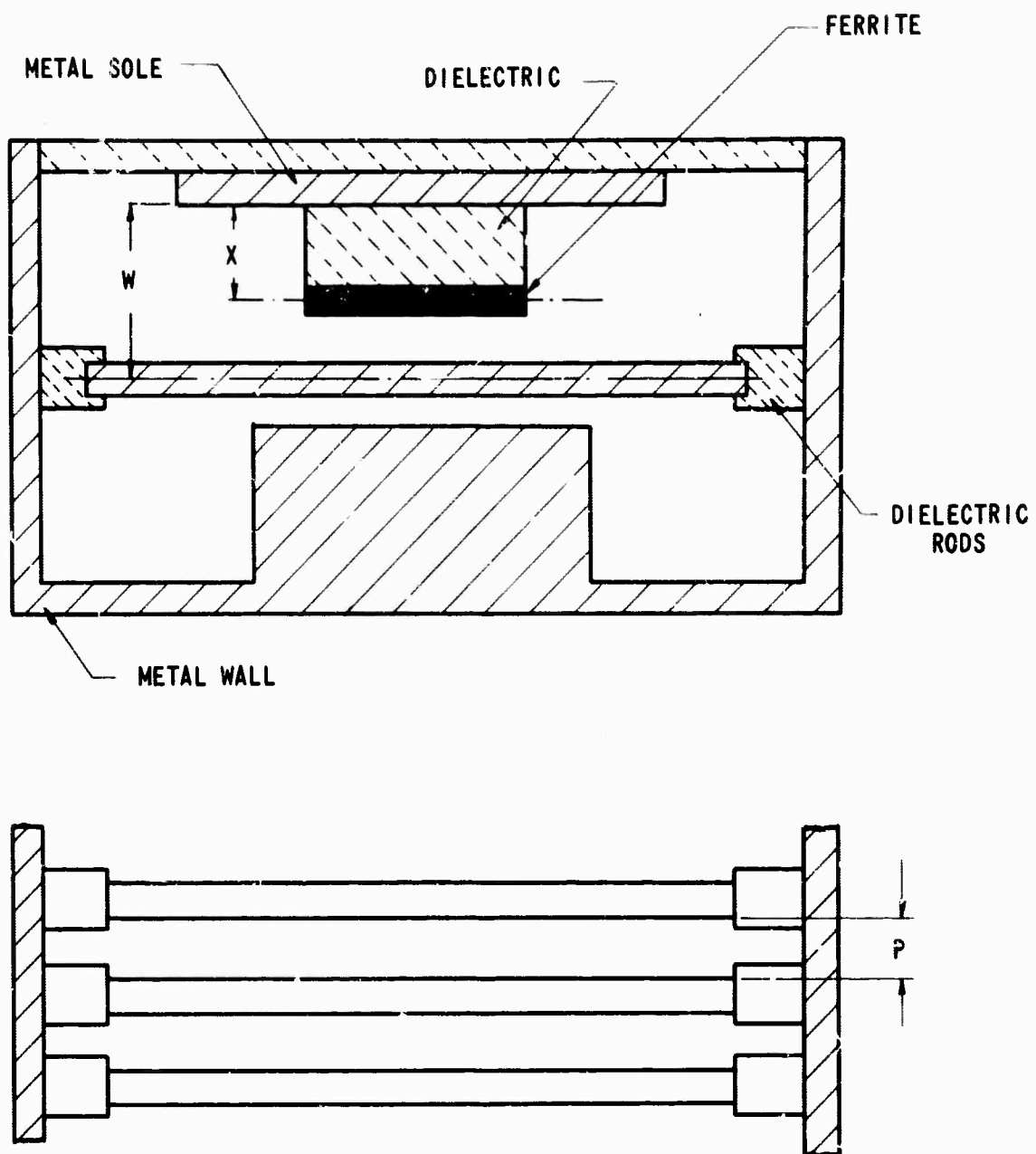
$$\text{Helix attenuation, } \alpha_{(\text{db/cm})} = 0.230 (\Delta x) \left(\sinh \frac{3.5 x_0}{w} \right) \quad (3-2)$$

where Δx is in centimeters.

Neglecting the effect of dielectric loading, one can expect that there will be an optimum x_0/w location for the ferrite at which the backwall is sufficiently distant to permit nearly circular polarization. At the same time, the delay line should be sufficiently removed from the ferrite so that coupling to higher order delay line harmonics does not take place. The observed data in this and in previous reports generally confirm this expectation in terms of optimum front-to-back ratios.

In the case of the Amplitron studies, annular discs of narrow linewidth ferrite were located adjacent to the strapped-vane delay line of the QKS1267 S-band Amplitron (Figure 3-2). This tube is rated at 60 kw peak power, 3% duty cycle, 16 db gain in the band 2.9 to 3.1 GHz. At the band-edge, as the pulse voltage rises through the synchronous range, difficulties are encountered from voltage tunable oscillations enhanced by regenerative circuit feedback and regenerative electronic feedback through the tube's drift space. The intent of the ferrites is to reduce the circuit feedback selectively so that low losses are obtained in the rated frequency band and high bilateral losses are obtained at the band-edge frequencies (slightly below 2.9 GHz).

The ferrites chosen for the band-edge application were Raytheon yttrium-iron garnets with $4\pi Ms \approx 1750$ and a linewidth of ~60 oersteds. Promising results have been obtained thus far.



648609

Figure 3-1 Meanderline Cross-Sectional View

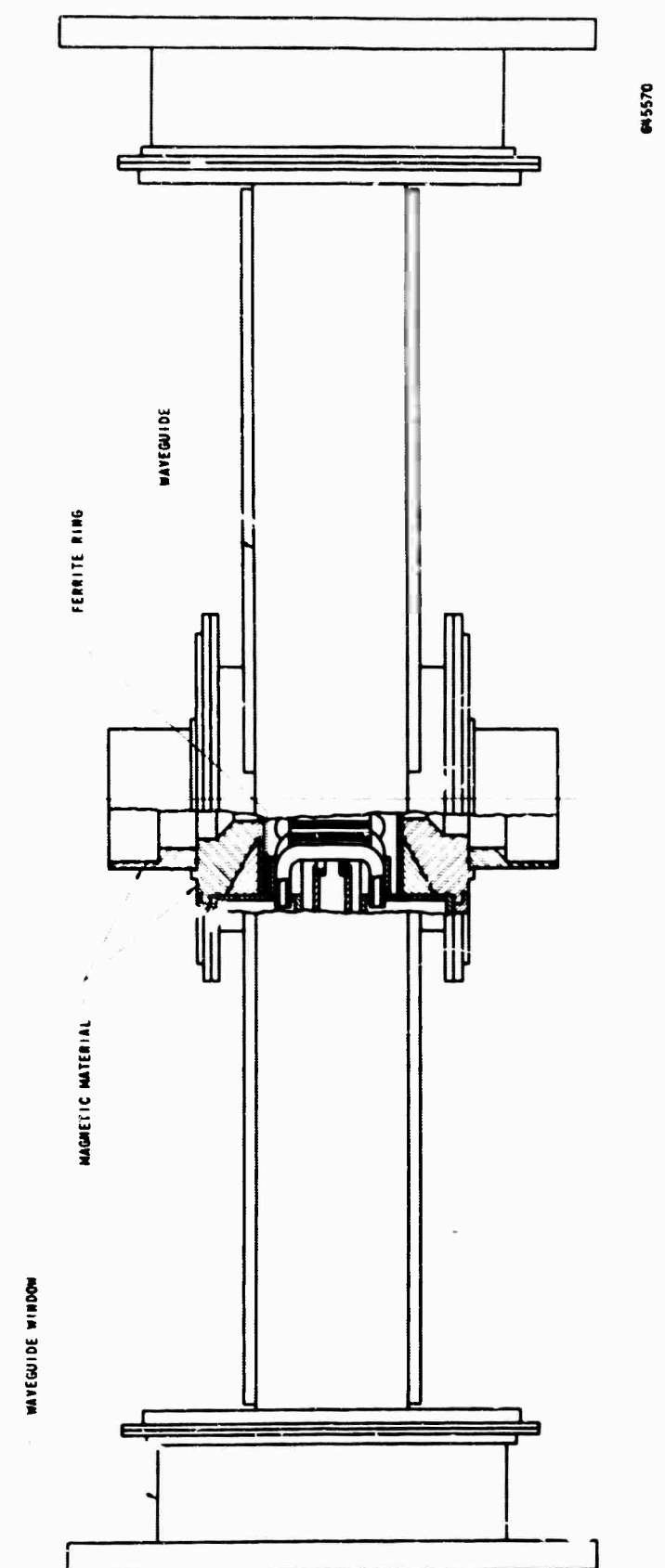


Figure 3-2 QKS1267 Delay Line Assembly (With Ferrite Ring)

The cold test program was directed into the following areas.

1. Improvement of the helix match to assure more easily interpretable data.
2. Measurements of the effect of ferrite on fast mode propagation.
3. Study of the effect of a metal base for the ferrites.
4. Study of the effect on bandwidth of higher magnetic fields.
5. Testing of the concept of oil-immersed ferrites.
6. Measurements of forward and backward losses for ferrites when used on ceramic bases of dielectric constants 3.0 and 6.0.
7. Cold test of the effect of narrow linewidth bodies in damping band-edge oscillation in Amplitrons.

As in previous tests, measurements were made with conventional reflectometer setups. Because this equipment is not designed for accuracy below 2% voltage transmission, an upper limit of 30 db backward loss is imposed by the equipment. Loss values were determined by comparison of the transmissions in (a) the loaded line, and (b) the unloaded line.

3.1 Cold test results. To obtain more accurate and meaningful loss measurements, particularly for forward-wave cases, considerable effort was expended in improving the coaxial-line-to-helix match. By insertion of a 5-section taper of the delay line pitch adjacent to the junctions, and by modifications of the junctions themselves, a distinctly improved match was achieved. Further improvement was obtained by placing dielectric loading in regions of the tapered section. Figure 3-3 shows the final match as measured with a resistive termination on the helix starting at the junction of the smooth line and the tapered end section. Figure 3-4 shows the data obtained when the termination was started at the axial center of the structure. A comparison of the two indicates the probability of incidental mismatches arising from mechanical imperfections of the line.

Because hot test vehicles now in the planning stage are being designed with ferrite base materials of either beryllia or boron nitride, the cold tests were conducted using dielectric bases having comparable dielectric constants, 6.0 and 3.0 respectively. For an $\epsilon'/\epsilon_0 = 3.0$, the backward losses obtained for various x_0/w positions are given in Figure 3-5. The associated forward losses are shown by Figure 3-6. Figures 3-7 and 3-8 present similar data for ferrites mounted on the base of dielectric constant 6.0.

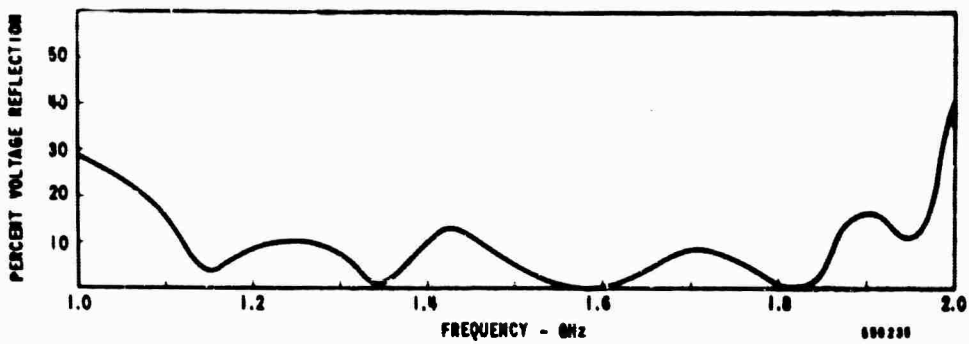


Figure 3-3 Percent Voltage Reflection Between Coaxial Input and Helix Line

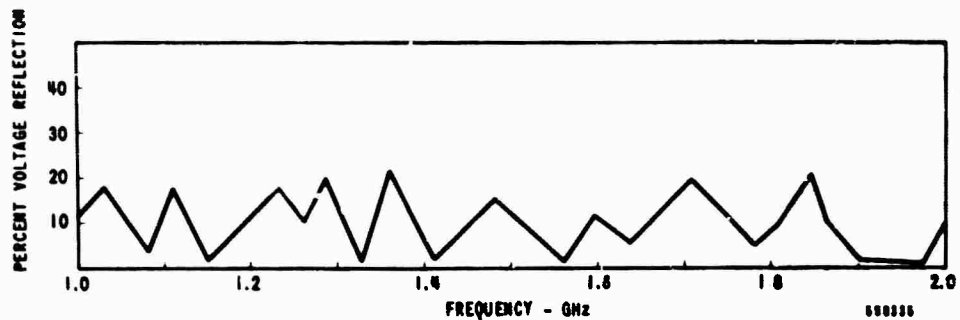


Figure 3-4 Impedance Match - Helix - Coaxial Inputs

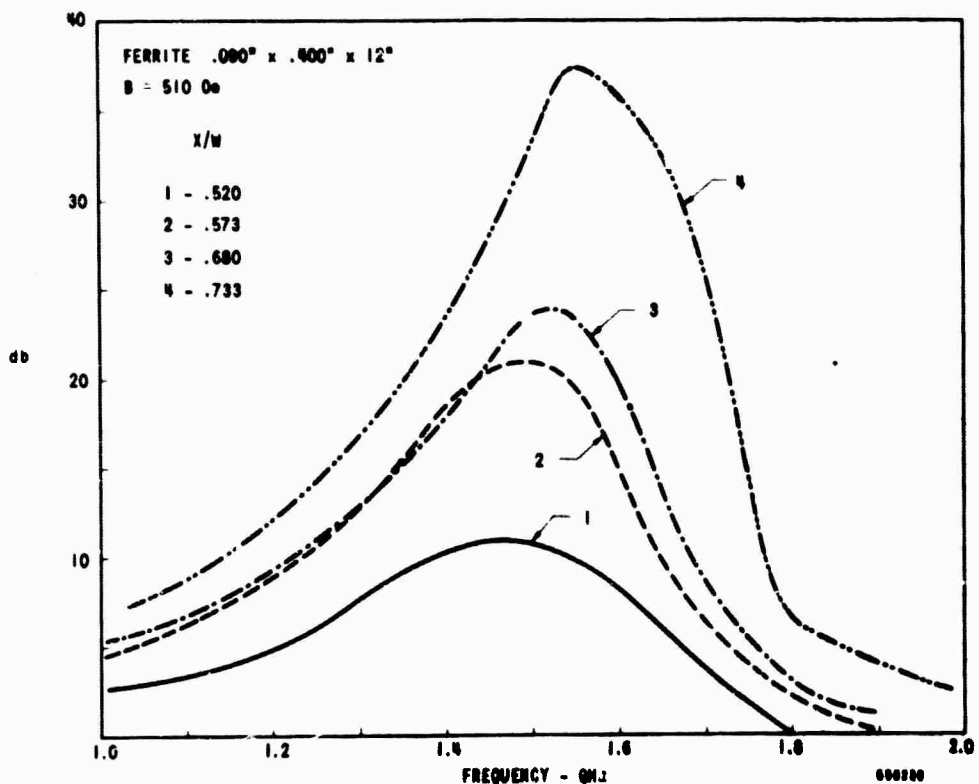


Figure 3-5 Helix - Backward Wave Power Loss (db)

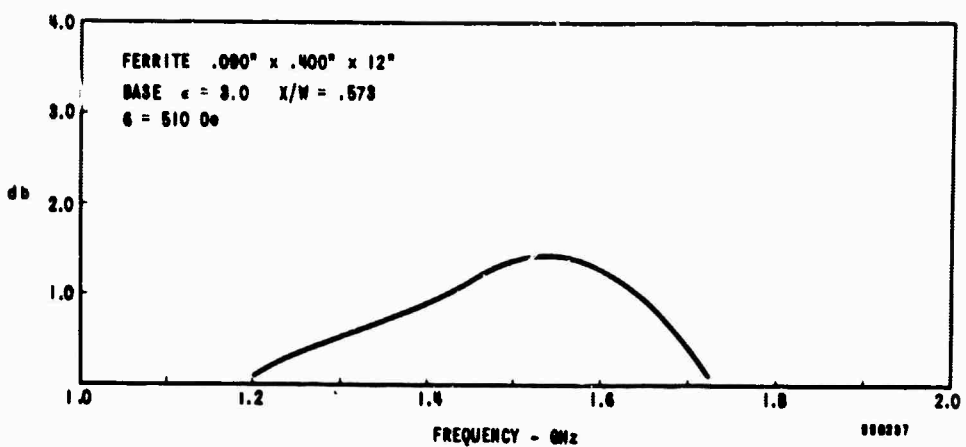


Figure 3-6 Helix - Forward Wave Power Loss (db)

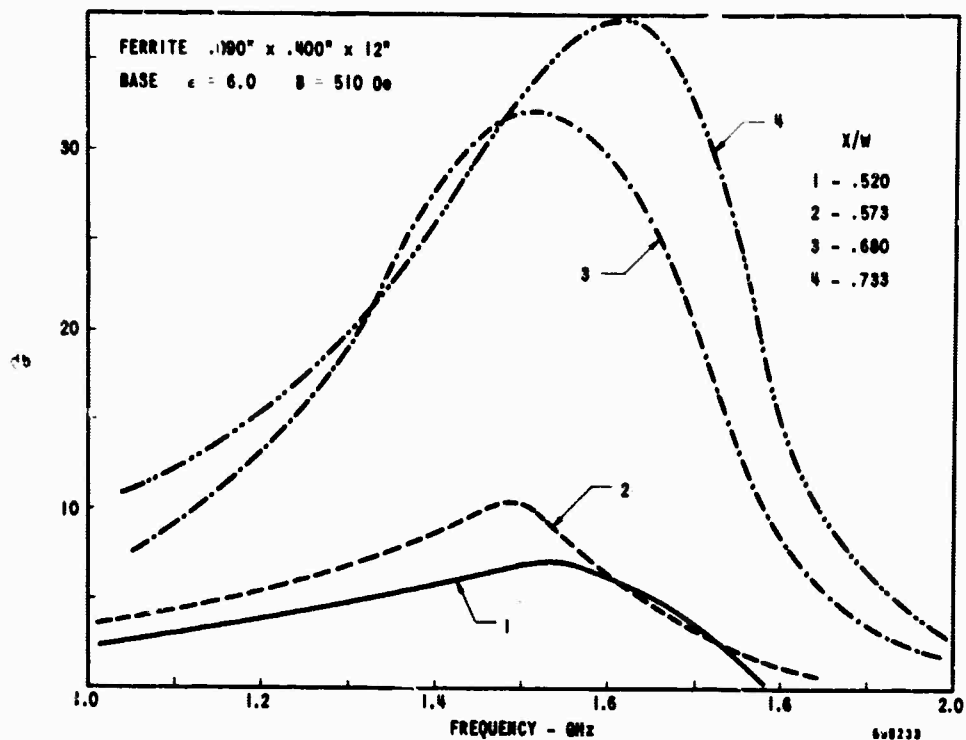


Figure 3-7 Helix - Backward Wave Power Loss (db)

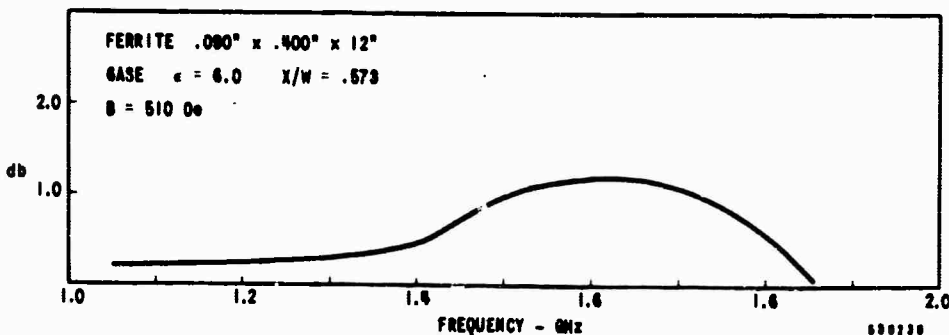


Figure 3-8 Helix - Forward Wave Power Loss (db)

Another set of experiments was conducted in which the dc magnetic field was varied since it had been experimentally observed that there might be a possibility of wider bandwidth at higher fields. Measured results are given in Figures 3-9 and 3-10 shewing backward losses for the ferrite sample mounted on materials of different dielectric constants. No significant change of bandwidth was found as a result of higher magnetic fields.

Because of the obvious bonding problem simplification which might be gained if the ferrite could be mounted on a metallic base rather than on dielectric, experiments were performed to determine feasibility. Promising results were not expected because of the deleterious effect of the metallic base upon the polarization of the magnetic fields. Observed data are given in Figure 3-11 for various x/w ratios, and forward-wave losses are given in Figure 3-12. Although the results are poor by comparison with data from dielectric-mounted ferrites, they indicate that some preferential loss is obtainable, perhaps enough to suffice for early hot testing.

In setting up the ferrite-on-metal experiments, samples were made up in which grooves were cut in the metal surface adjoining the ferrite, running longitudinally in one case and transversely to the direction of wave propagation in the other case. These slots, 0.050-inch wide on a pitch of 0.090 inch, and 0.050 inch deep were intended to induce better circular polarization of the rf magnetic fields. The results of these tests appear in Figures 3-13 and 3-14. In the case of Figure 3-13, curve no. 3 for an x/w spacing of 0.680 inch appears anomalous and worthy of recheck. Forward losses for the ferrite on grooved metal bases were generally similar to those observed with ungrooved bases.

Another approach toward relief of the bonding and heat transfer problems would consist of encasing the ferrite in a dielectric chamber outside the vacuum envelope and integral with the normal coolant chamber of the device. Figure 3-15 indicates one possible configuration. Here the sample used for cold test was immersed in Univolt 33 oil. In an actual tube, the oil coolant would be caused to flow across all ferrite surfaces to remove heat. Figures 3-16 and 3-17 show forward and backward losses observed with the ferrite-in-oil model. It will be seen that addition of the dielectric cover and oil to the chamber caused the forward losses to increase. The stycast cover is believed to be the chief contributing factor to this greater loss.

Crossed-field devices are often plagued by spurious phenomena such as (1) cyclotron wave interaction with fast modes or (2) fast mode feedback into circuit input or the gun. These fast modes are inherent in the crossed-field device because of its insulated sole electrode, and their suppression is often a major problem. To study these modes, a four-port helix network was constructed as indicated in Figure 3-18. The entire assembly was shielded to inhibit radiation of the fast modes. Measured results for this helix assembly are presented in Figures 3-19 and 3-20. The former shows transmission from port 2 to port 4 without magnetic field and indicates that the sole-helix geometry can readily support rf propagation over the entire band. As expected, the application of dc magnetic field had little effect since the rapid modes do not couple to the ferrite in its "normal"

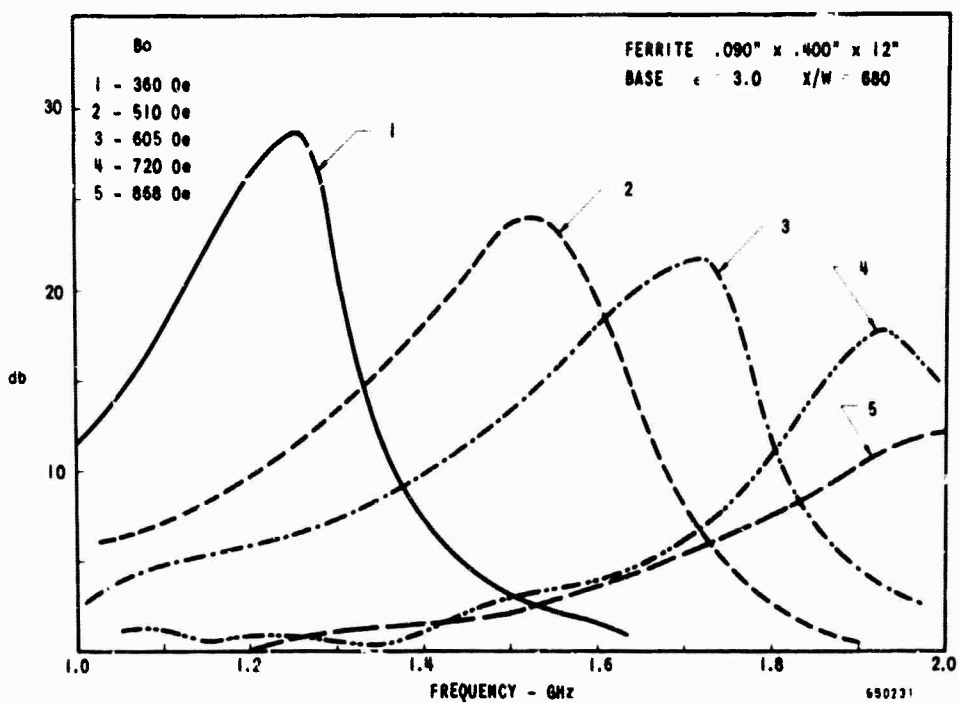


Figure 3-9 Helix - Backward Wave Power Loss (db)

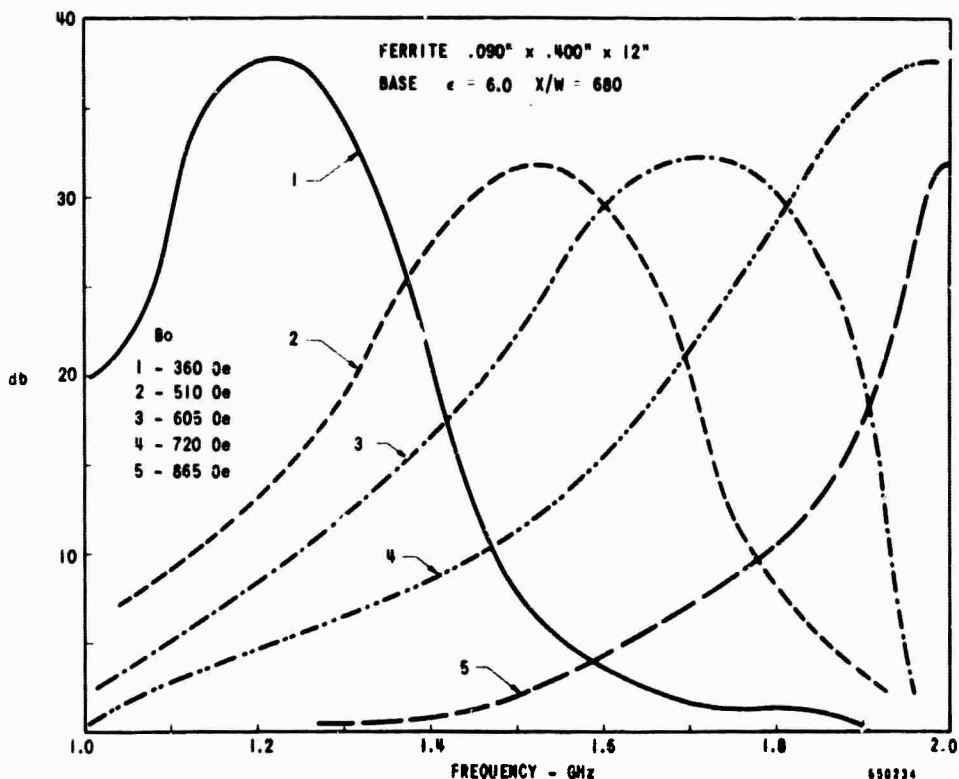


Figure 3-10 Helix - Backward Wave Power Loss (db - B_0)

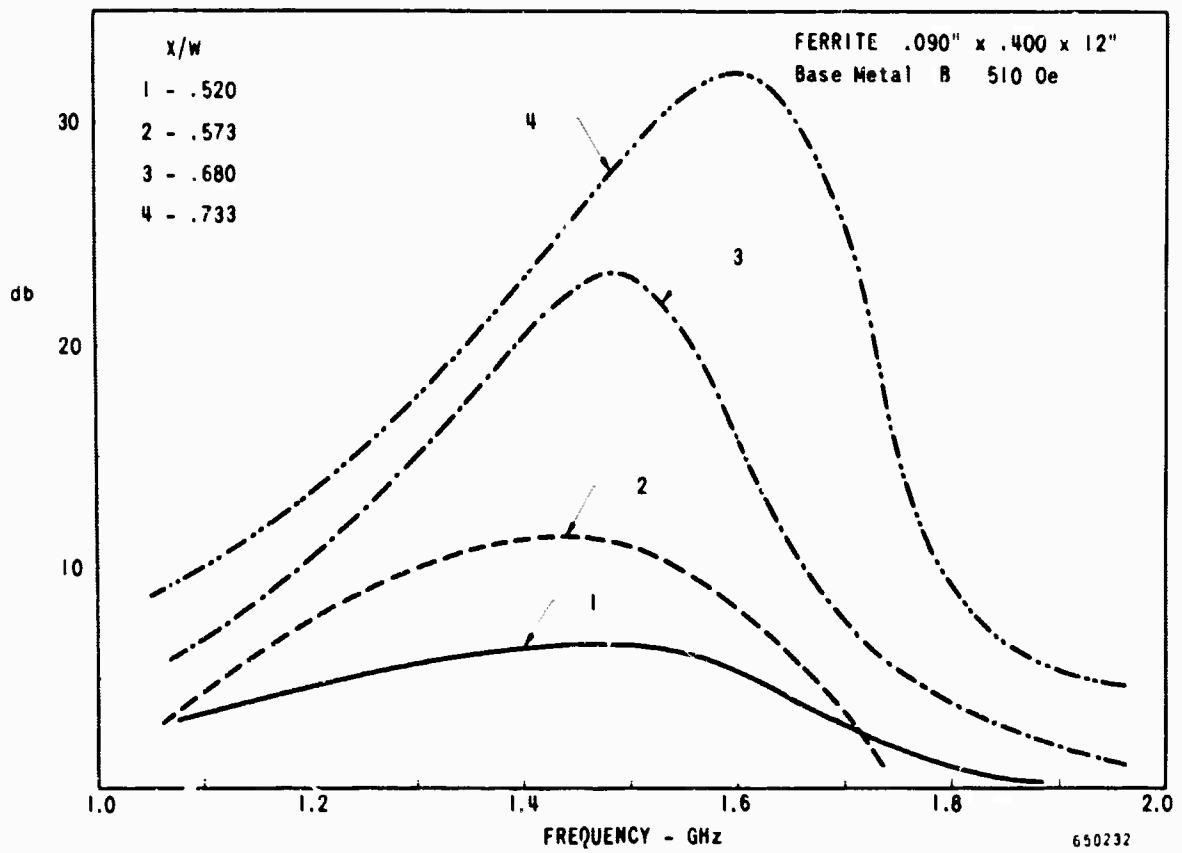


Figure 3-11 Helix - Backward Wave Power Loss (db - X/W)

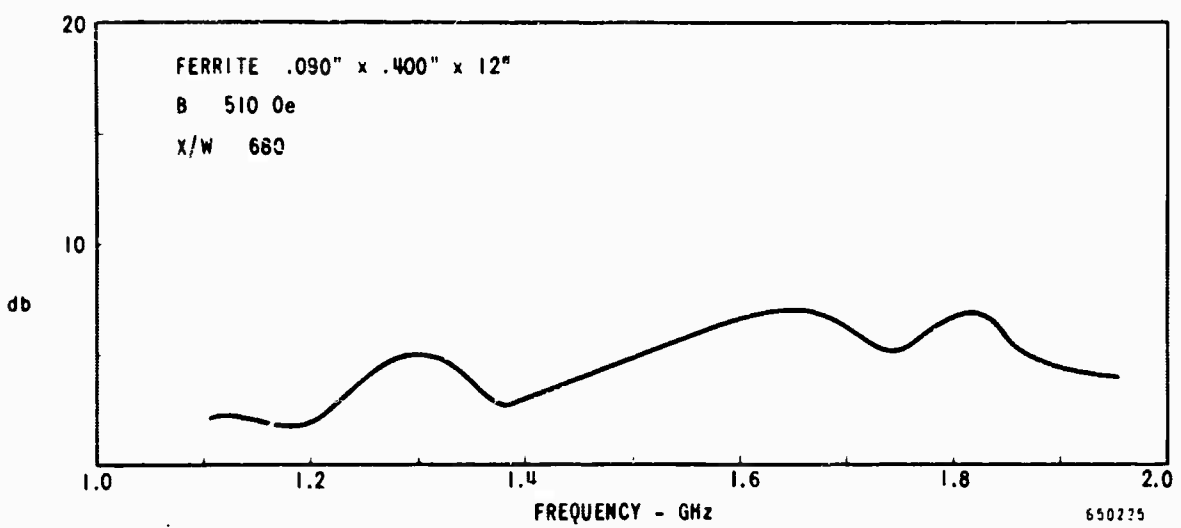


Figure 3-12 Helix - Forward Wave Power Loss (db)

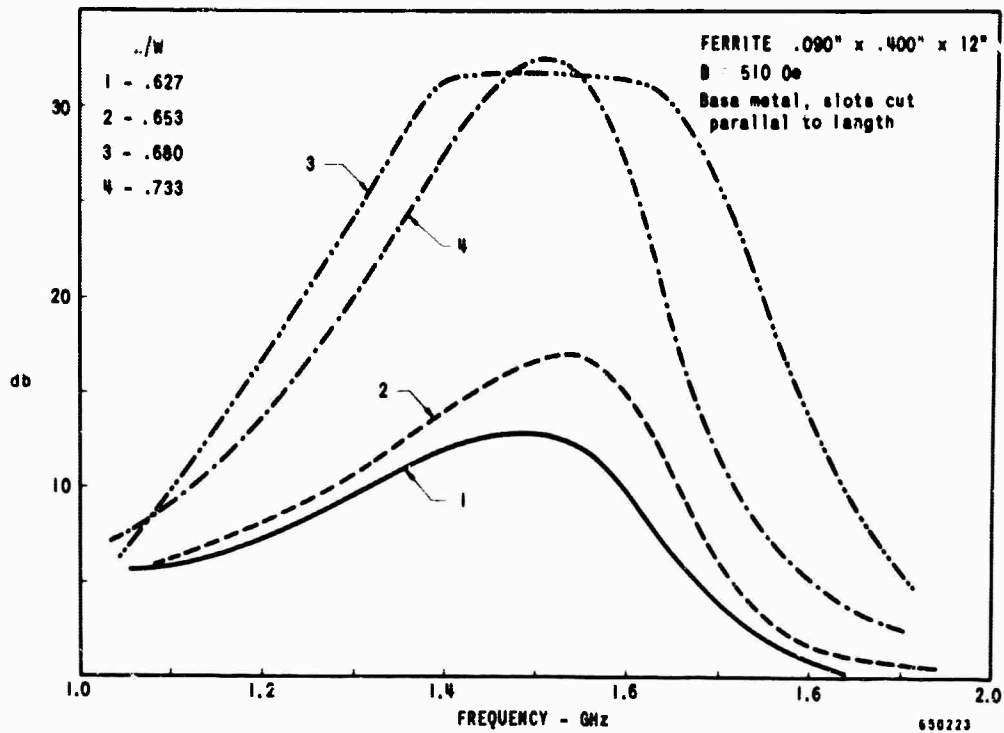


Figure 3-13 Helix - Backward Wave Power Loss (db)

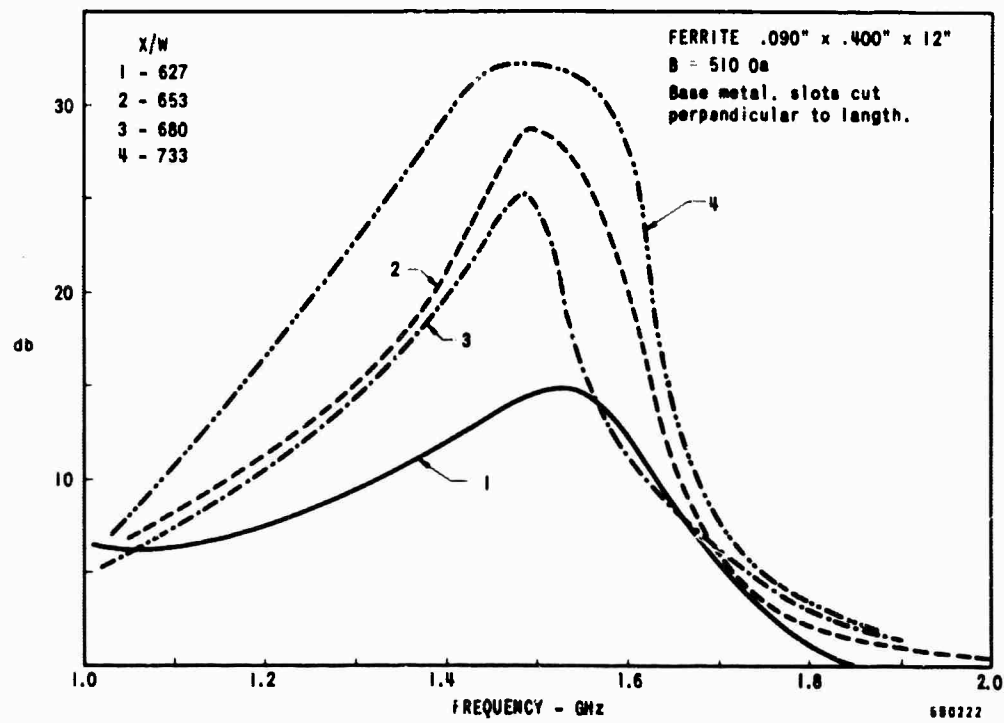


Figure 3-14 Helix - Backward Wave Power Loss (db)

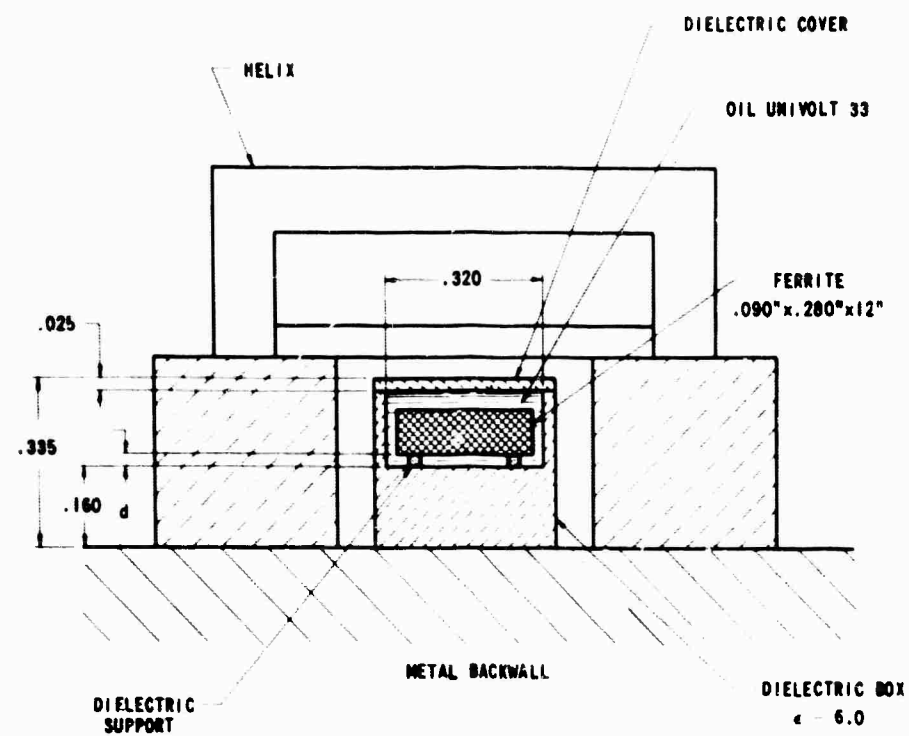


Figure 3-15 Dielectric Box and Ferrite for Helix Delay Line
(12" long)

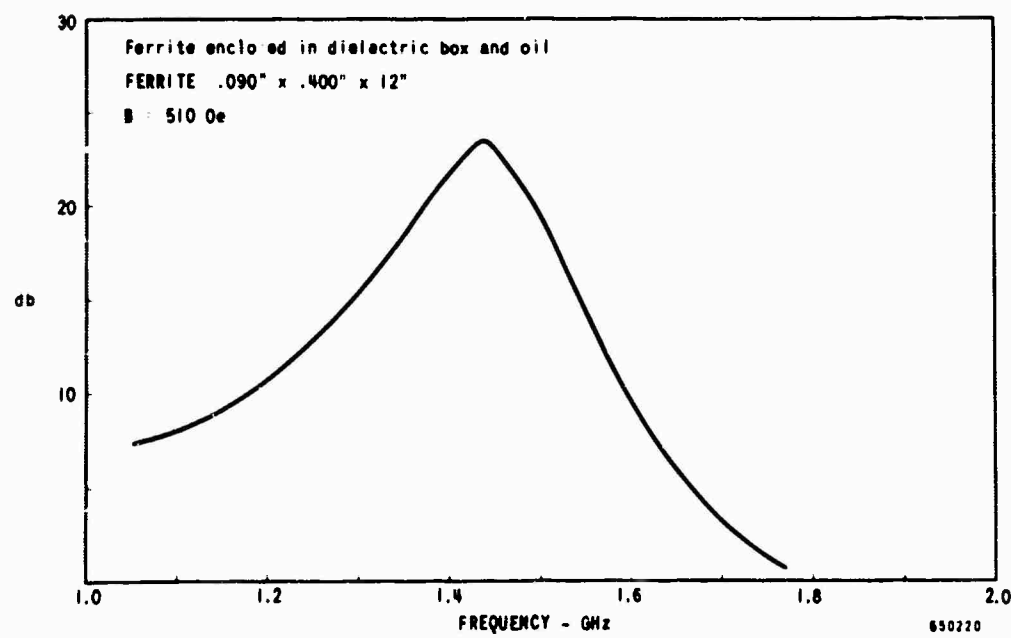


Figure 3-16 Helix - Backward Wave Power Loss (db)

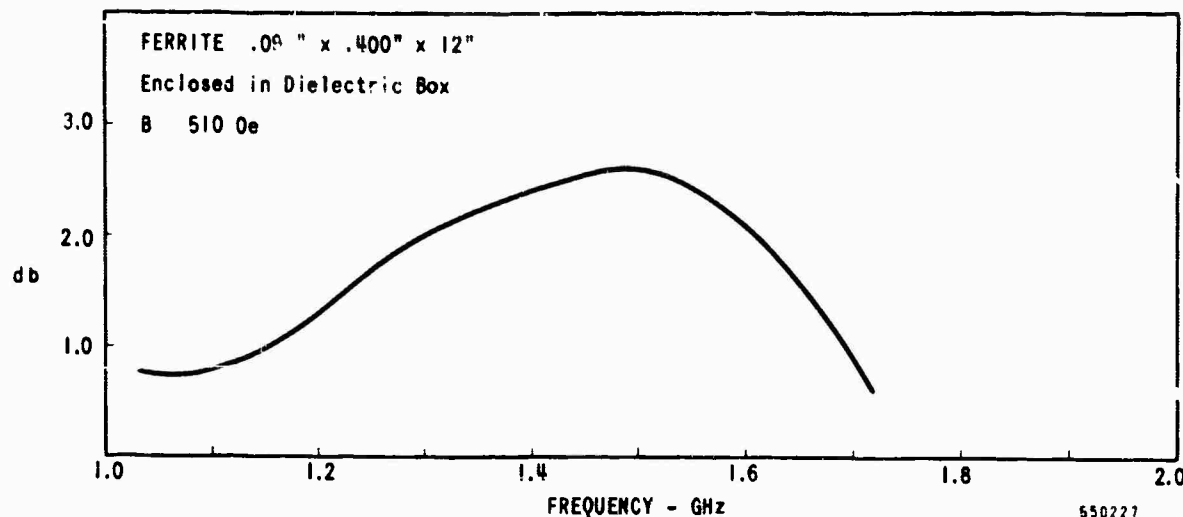


Figure 3-17 Helix - Forward Wave Power Loss (db)

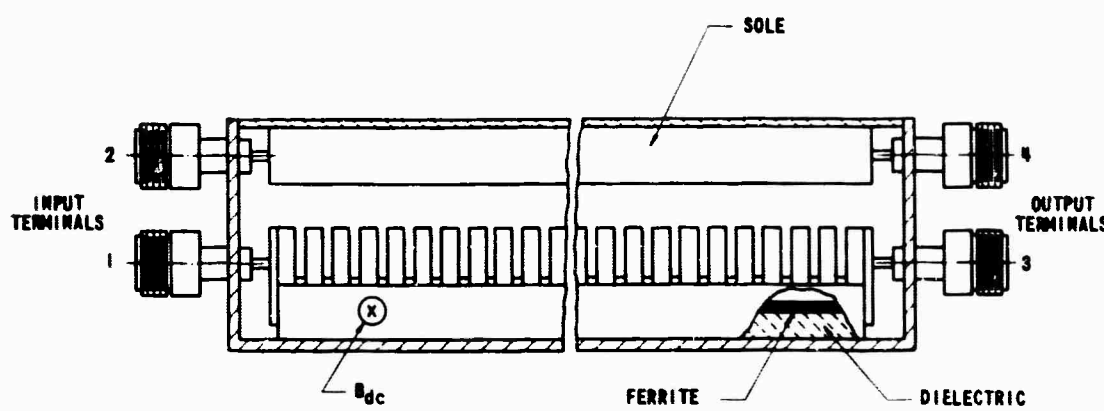


Figure 3-18 Helix Delay Line - 4 Terminals
Cross-Sectional View



Figure 3-19 Percent Voltage Transmission (Port 2 to 4)

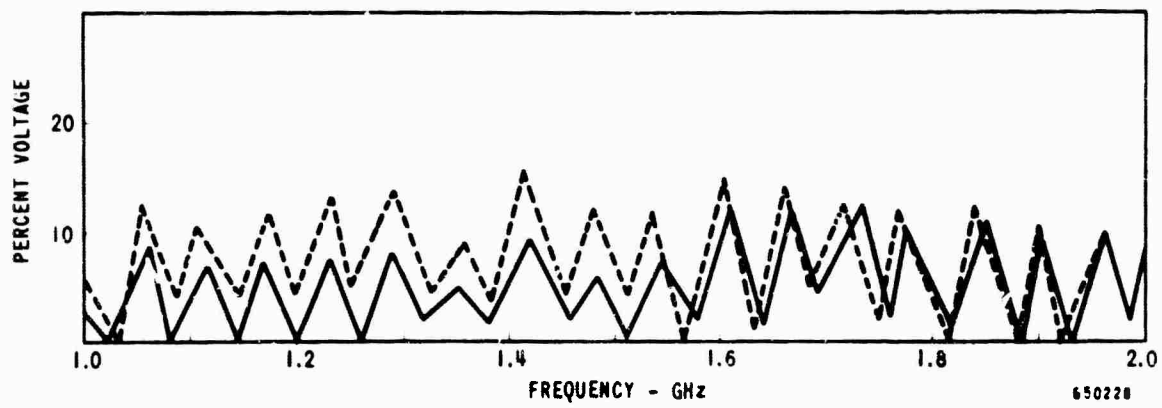


Figure 3-20 Helix - Percent Voltage Transmission from Port 1 to 4

location. In the latter, Figure 3-20, transmission from port 1 to port 4 is shown. In this case, appreciable helix-sole coupling was observed over the entire band and again the ferrite was ineffective in damping this type of transmission.

The helix measurements are summarized in Table 3-1. The following comments are applicable.

1. Loss measurements reported for this quarter are more accurate because of the improvements secured in the rf match.
2. Both forward and backward losses are generally insensitive to the dielectric constant of the dielectric support, but the forward losses are slightly greater for a support $\epsilon'/\epsilon_0 = 6.0$.
3. The optimum location for the ferrite is for $x = 0.215$ inch and $x/w = 0.573$ inch.
4. No appreciable increase of bandwidth was achieved at the higher magnetic fields.
5. Although the front-to-back ratio deteriorates when a ferrite is used with a metallic base, such a base may have some usefulness.
6. The inclusion of slots in the metallic base has no appreciable effect on the results.
7. From Table 3-1 it can be seen that the addition of oil and a dielectric chamber increases the forward losses by 1.0 db. This increased loss is attributed primarily to the dielectric cover of the box and could be reduced by moving the ferrite an additional 0.015 inch from the helix.

3.2 Cold tests - ferrites in the Amplitron. Most Amplitron tubes utilize the backward-wave fundamental waves of a bandpass filter type of delay line. These tubes are customarily built to be very short electrically to minimize circuit losses and therefore achieve the high efficiency characteristic of the device.

High gain Amplitrons, i. e. those having gain capability in the order of 20 db, can be and sometimes are plagued by feedback oscillations at their lower band-edge (near the network cutoff frequency). Here there is an inherent reflection at each end of the delay line which, coupled with the low loss and electronic feedback across the tube's drift space, leads to spurious oscillation. The frequency determining element for this oscillation is the backward-wave set up when the voltage is proper for synchronous conditions at the band-edge. Thus, in a pulsed tube, the voltage rises until synchronism occurs at a frequency for which the input voltage reflection

Table 3-1. Summary of Peak Loss Values for Helix

L_f , L_b = peak forward and backward losses.
 f_1 , f_b = frequencies at which peak occurred.
 Length of ferrite = 12 inches.
 Spacing of helix to back wall $w = 0.375$ inches.

Sample Size inches	Dielectric Constant of Substrate	Average Position x_0 inches	x_0/w	Σ Gauss	Measured			
					f_1 GHz	L_f db	f_b GHz	L_b db
0.090x 0.400	$\epsilon = 3.0$.195	.520	510	1.5	<.5	1.45	11.0
		.215	.573	"	1.53	1.4	1.50	20.7
		.255	.680	"	1.55	1.9	1.52	24.0
		.275	.783	"				
0.090x 0.400	$\epsilon = 6.0$.195	.520	510	1.5	0.7	1.49	7.0
		.215	.573		1.60	1.1	1.50	11.0
		.255	.680		1.64	8.2	1.52	32.0
		.275	.783		1.65	7.5	1.64	37.5
0.090x 0.400	$\epsilon = 3.0$.255	.680	360	1.260	1.15	1.260	28.8
				510	1.55	1.9	1.525	24.0
				605	1.65	2.3	1.715	21.7
				720	1.93	7.2	1.825	16.7
				865	--	--	+2.0	--
0.090x 0.400	$\epsilon = 6.0$.255	.680	360	1.280	5.4	1.225	38.0
				510	1.60	8.2	1.525	32.0
				605	1.775	12.2	1.700	32.0
				720	+2.0	19.0	1.960	37.5
				865	--	--	+2.0	--

Table 3-1. Summary of Peak Loss Values for Helix (continued).

Sample Size inches	Dielectric Constant of Substrate	Average Position x_0/w inches	x_0/w	B Gauss	Measured			
					f ₁ GHz	L _f db	f _B GHz	L _b db
0.090x 0.400	Metal	.195	.520	510	1.5	4.5	1.45	6.5
		.215	.573		1.5	1.35	1.44	11.8
		.255	.680		1.5	3.0	1.485	23.5
		.275	.733		1.725	6.7	1.60	32.0
0.090x 0.400	Metal - Slcts cut parallel to length	.235	.627	510	1.62	1.9	1.50	12.7
		.245	.653		1.625	2.4	1.54	17.3
		.255	.680		1.615	11.4	1.50	51.8
		.275	.733		1.635	5.6	1.52	32.0
0.090x 0.400	Metal - Slots cut perpendi- cular to length	.235	.627	510	1.635	2.0	1.525	14.8
		.245	.653		1.635	3.4	1.49	29.0
		.255	.680		1.60	3.3	1.485	25.5
		.275	.733		1.60	5.7	1.500	32.0
0.090x 0.280	Ferrite in Dielectric Box, Note 1	.280	.747	510	1.625	3.3	1.435	28.3
0.090x 0.280	Ferrite in Dielectric Box, Note 2	.280	.747	510	1.435	4.3	1.460	28.5
0.090x 0.280	Ferrite in D lectrice Box, Note 3	.260		510	1.585	2.7	1.435	23.8

Note 1 No oil or dielectric cover or Box. d = 0.025"

Note 2 As shown in Figure 3-15: d=0.025 "

Note 3 As shown in Figure 3-15: d=0.010"

coefficient is about 70%. Backward-wave oscillation power is then observed at the tube output, and, as the voltage rises further, the external spurious power increases. When synchronism reaches the point at which the input reflection coefficient has dropped to about 20%, then the circuit/electronic feedback is no longer sufficient to sustain oscillations and the tube then begins to amplify properly.

Because the voltage tunable oscillations at band-edge frequencies can cause interference with other radars, it is desirable to eliminate them insofar as possible. Under some circumstances, the amount of electronic feedback through the drift space can be altered enough to damp these oscillations. When this is impractical, the possibility of reducing the feedback by means of selective loss must be evaluated. However, because both the spurious waves and the amplification process are backward-wave phenomena, the use of unidirectional loss cannot be considered. On the other hand, a narrow-band ferrite offers attraction in the sense that it may provide high loss at the band edge and low loss in the band of interest. In this type of application, selectivity is obtained solely through frequency selectivity, and bilateral loss is perfectly acceptable.

A need for ferrite damping having arisen in connection with an S-band pulsed Amplitron, the QKS1267, cold tests were performed to study the possibility of highly selective damping using a ring of ferrite adjacent to the tube's delay line. The geometry is illustrated in Figure 3-2. It was desired that the ferrite loss peak at 2850 MHz, the point of 50% input reflection coefficient, when a field of 2400 gauss was applied.

Three ferrite rings were checked as follows:

Material, Raytheon type R-171

- (a) 1.700" OD x 1.130" ID x 0.050" thick
- (b) 1.600" OD x 1.130" ID x 0.040" thick
- (c) 1.560" OD x 1.130" ID x 0.030" thick

Using these discs, the dc magnetic field for ferromagnetic resonance occurred at too low a gauss level. To increase the resonant field, thinner samples were made and tested and, in addition, the magnetic field shape (orientation) was improved by flattening the pole pieces. The net effect was to bring the resonant field closer to the field present in the operating tube. At this time there is still some discrepancy between the two field values but it appears feasible to eliminate this difference.

It should be realized, however, that when compatibility is achieved there are major potential problems which could prevent the success of the ferrite approach. Basically, these problems involve bonding and heat transfer. If the ferrite is fully effective in preventing the feedback oscillations from building up there will be little heat to dissipate. It is more likely to be only partially effective, however, and hence may be called on to dissipate considerable power. Therefore, a good bond is necessary and, since

unilateral loss is not necessary, a ferrite-to-metal bond should be acceptable. A moderate effort has been initiated, therefore, to learn more about seals of ferrite to metals, but, as of the time of writing, the effort had not produced tangible results.

4. SURVEY OF FERRITE MATERIALS

The survey started during the last period⁽¹⁾ was extended to include C-band (4.0 to 8.0 GHz).

The resonance condition in a ferrite slab as a function of shape, $4\pi Ms$, and applied magnetic field was plotted for $f_r = 6000$ MHz and $\gamma = 2.8$ using the method outlined in the previous report. The results are shown in Figure 4-1. They show that in order to obtain a form factor between 3 and 8, the $4\pi Ms$ can assume values ranging from 1500 g to 3000 g, the applied magnetic field being chosen between 1600 g and 2000 g. The nominal field for a C-band CFA is 1850 g.

It was established that a material with a high curie temperature is needed, and, if the assumption as to the behavior of the tube under high forward loss conditions is correct, with a broad linewidth. The class of NiFe spinels seems to answer the present needs.

Unfortunately, when substitutions are made to the material to decrease the $4\pi Ms$ and increase the linewidth, an increase of the gyro-magnetic ratio γ is observed. Most of the materials reviewed show a γ of the order of 3.55.

Accordingly, the curves giving the resonance conditions have been redrawn to show this change. They are given in Figures 4-2 to 4-5.

The effect of increasing γ is to decrease the field necessary for resonance if the slab form factor and the $4\pi Ms$ are kept constant. At the lower bands, this puts an additional restraint on the form factors that can be used to obtain resonance at the nominal field of the tube. In general, the ferrite slab will have to assume more of an H-plane geometry. This could be serious if all the heat transfer from the ferrite has to be made through a broad face.

At the present time, it is planned to place the slab in an oil bath outside the vacuum envelope so its exact shape loses some importance. Use of a ferrite made by Sperry under the name material #40 is being considered.

4.1 Evaluation of material #40 from Sperry Microwave Co. It has been shown that a ferrite material with a curie temperature as high as possible is needed, since the ferrite can be subjected to temperature of the order of 250°C during operation of the tube. In addition, if the assumption that appreciable cold insertion losses are acceptable is correct, broad linewidth can be tolerated in order to increase the bandwidth of the resonance curve without recourse to field shaping, staggering the demagnetization factors, or changing the $4\pi Ms$.

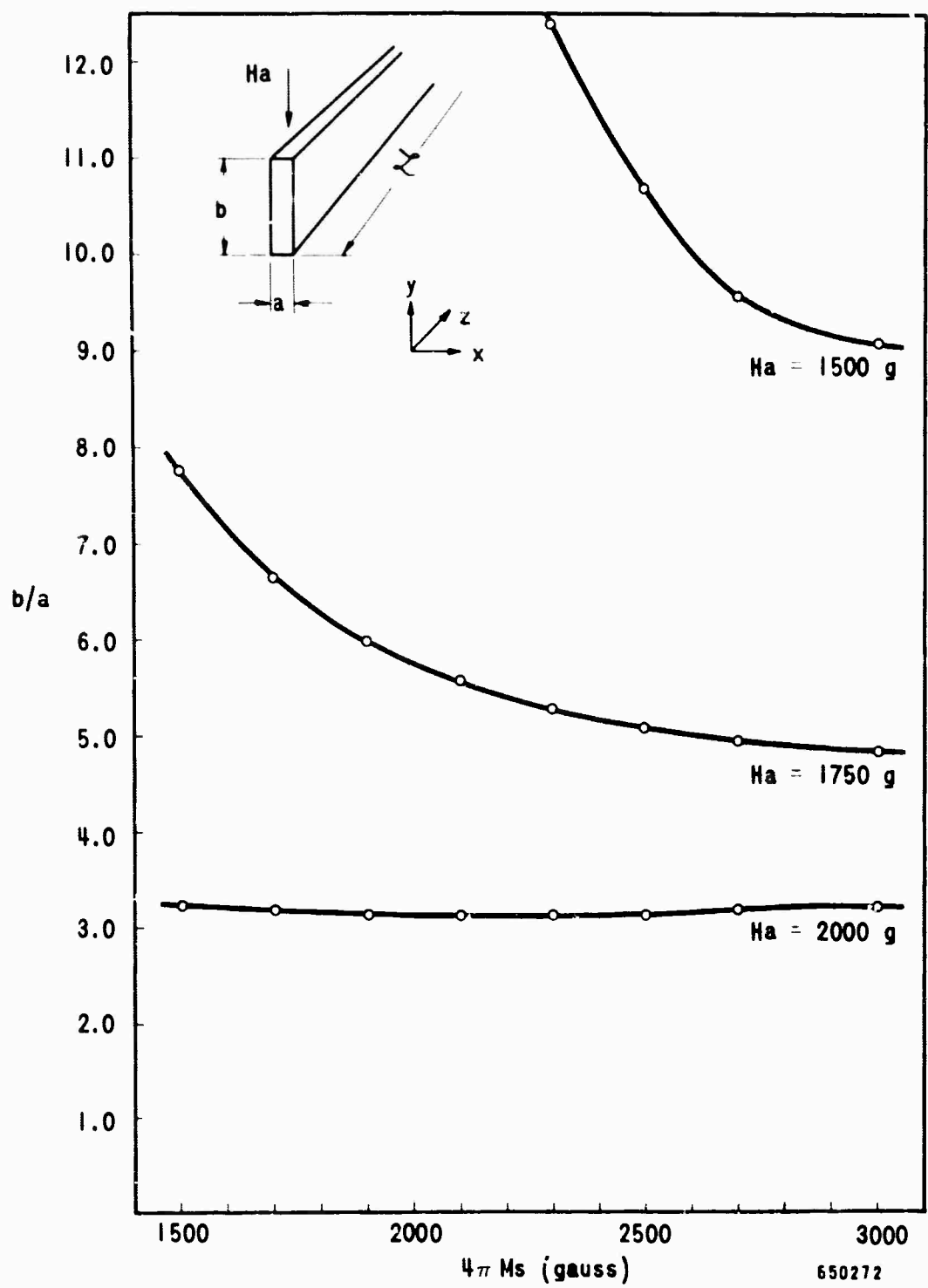


FIGURE 4-1 Resonance Condition $b/a = f(4\pi M_s, H_a)$
for $\omega_r = 6000$ MHz, $\gamma = 2.8$

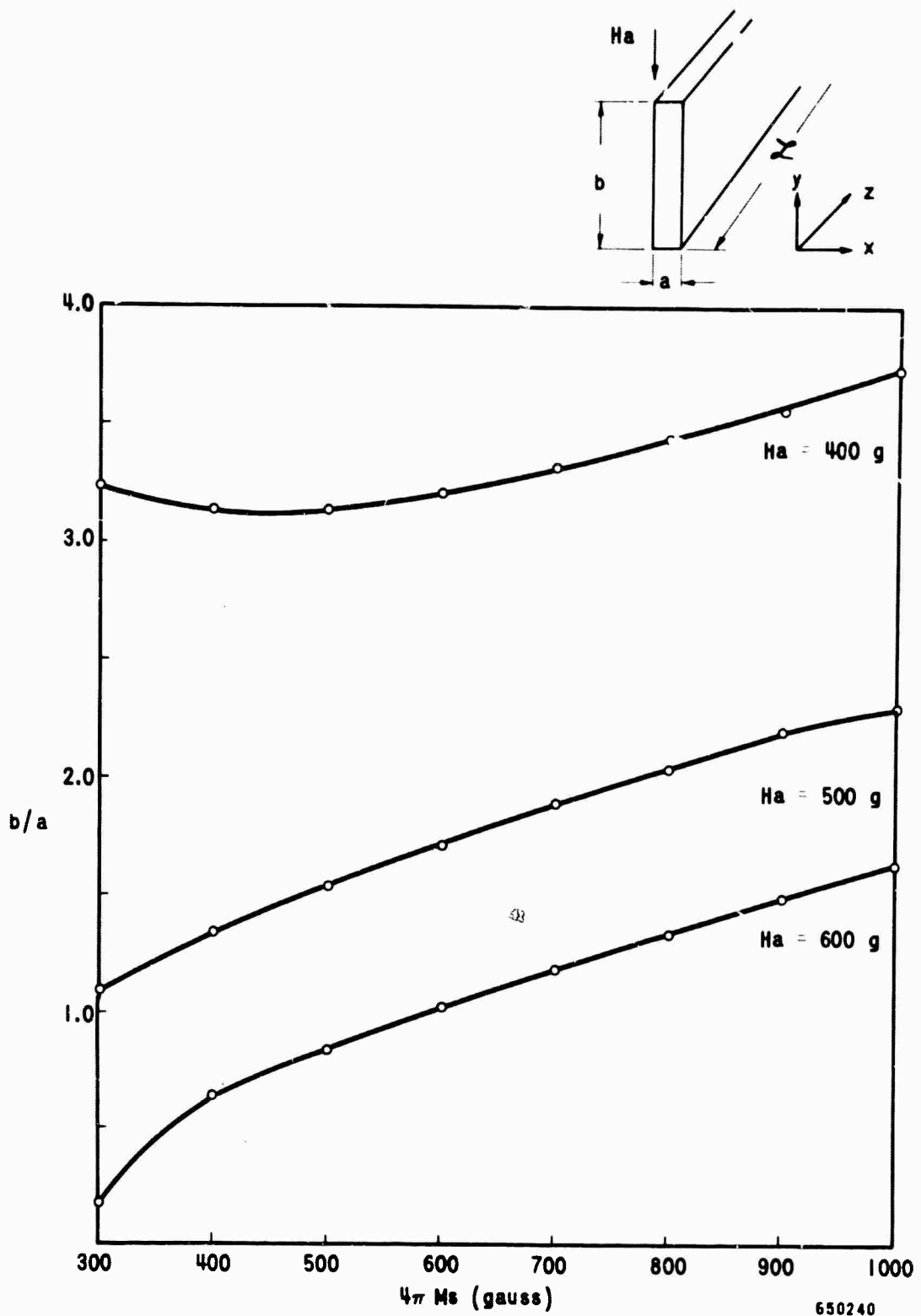


Figure 4-2 Resonance Condition b/a ($f(4\pi M_s, H_a)$)
for $\omega_r = 1500 \text{ MHz}$, $\gamma = 3.55$

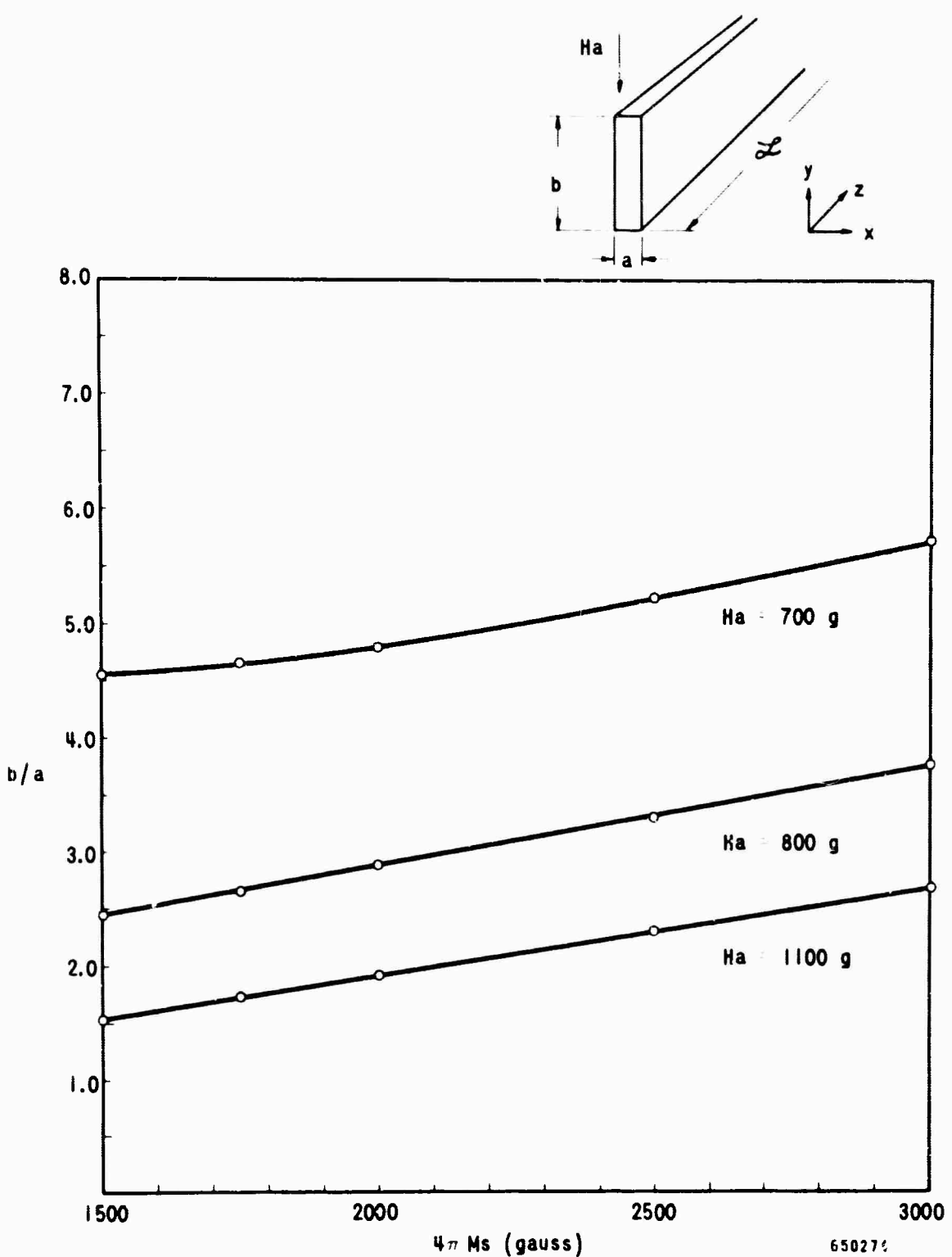


Figure 4-3 Resonance Condition $b/a = f(4\pi M_s, H_a)$
for $\omega_r = 3000$ MHz, $\gamma = 3.55$

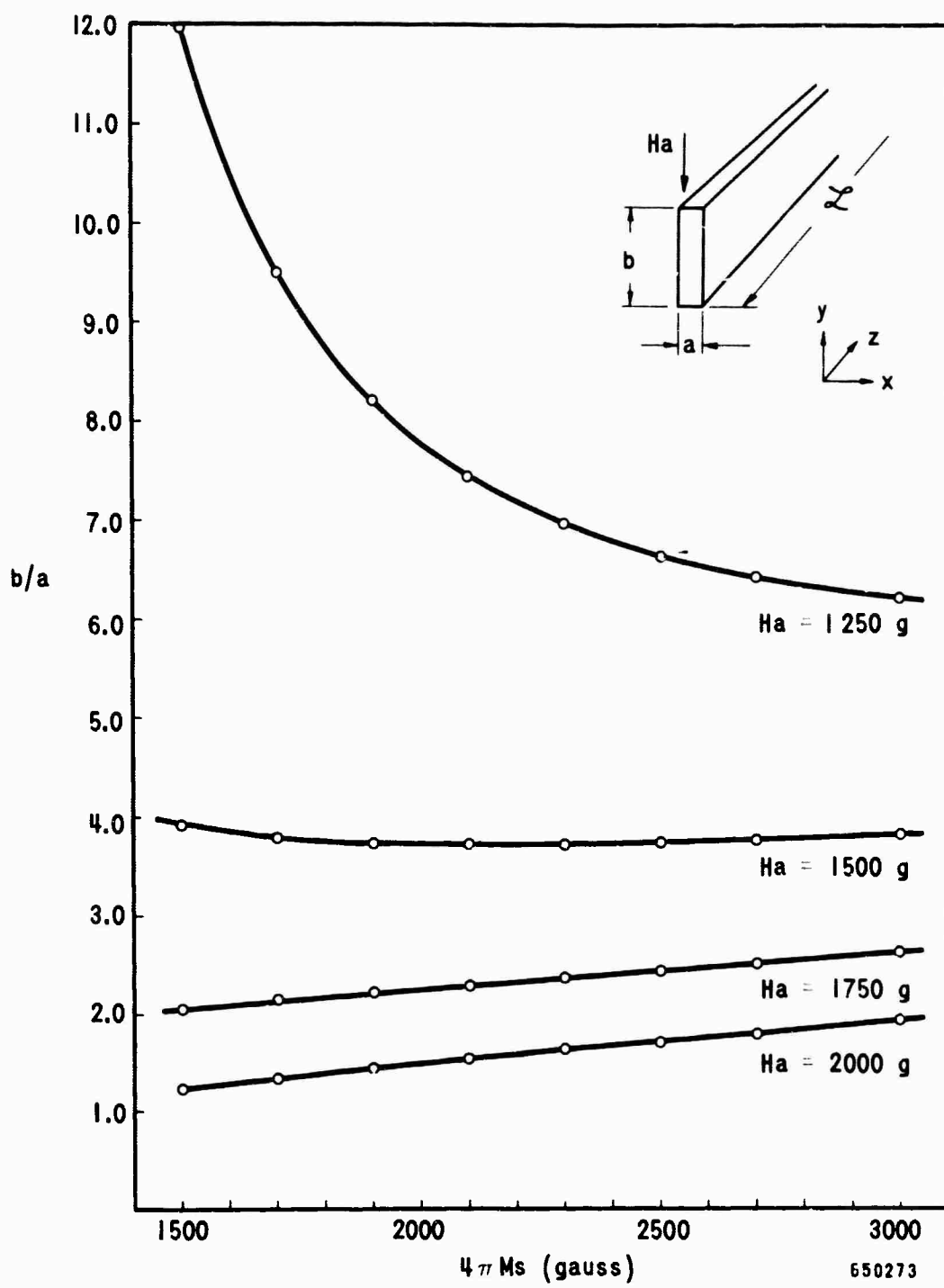


FIGURE 4-4 Resonance Condition $b/a = f(4\pi M_s, H_a)$
for $\omega_r = 6000 \text{ MHz}$, $\gamma = 3.55$

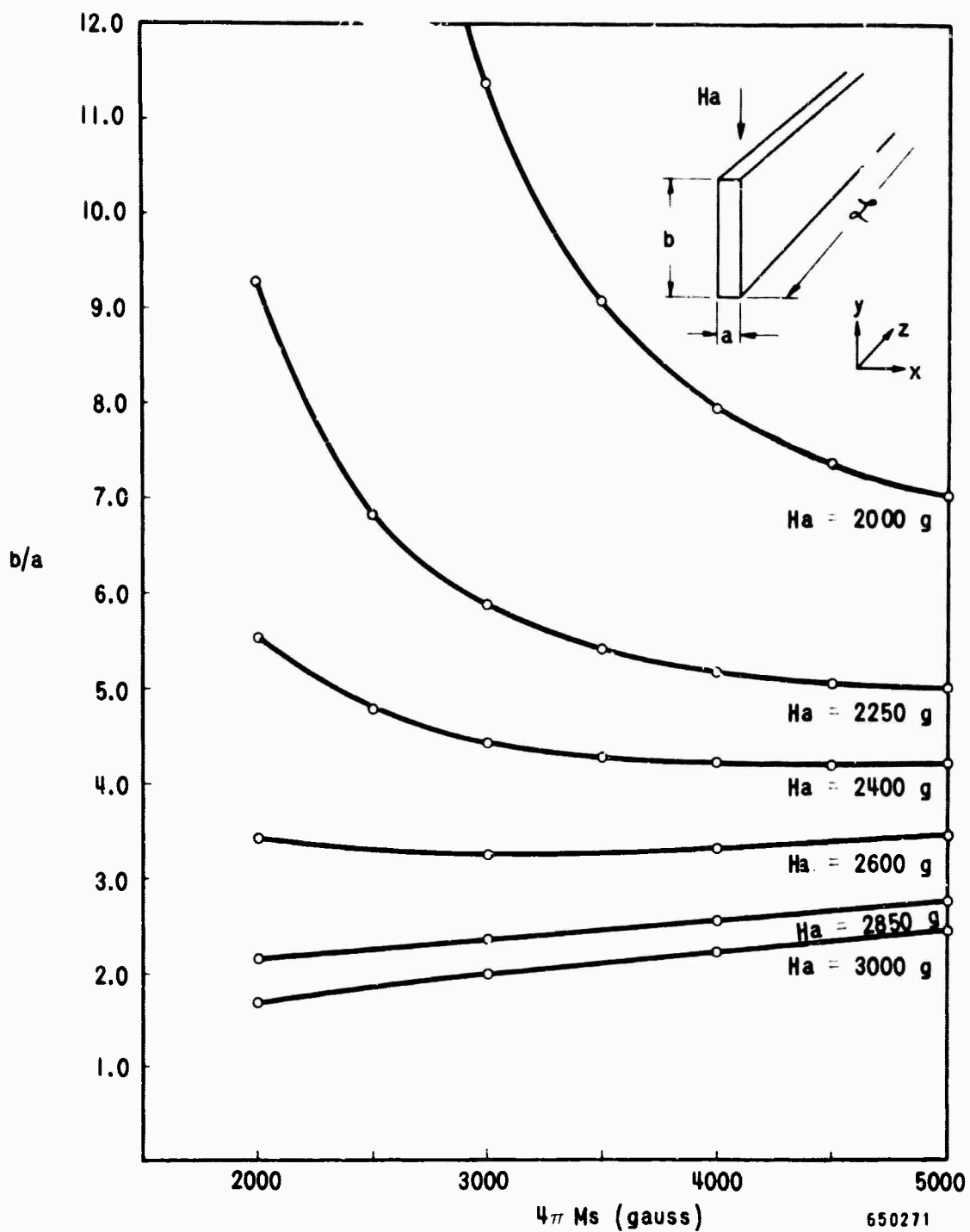


FIGURE 4-5 Resonance Condition $b/a = f(4\pi M_s, Ha)$
for $\omega_r = 10,000 \text{ MHz}$, $\gamma = 3.55$

Material #40, fabricated by Sperry Microwave Co., seems suited for use at S-band and possibly L-band. It is a nickel ferrite with additions of copper, cobalt, manganese and aluminum.

Its published characteristics are:

$4\pi M_s$	= 800 gauss
ΔH	= 600 oe
γ	= 4.13
T_c	= 370°C
$\tan \delta$	= 0.002

One bar of this material was procured and extensively measured.

At room temperature, the properties are:

$4\pi M_s$	= 841 g
ΔH	= 645 oe
γ	= 3.89
$\tan \delta$	= 0.0002
ϵ' / ϵ_0	= 12.1

The coefficient of thermal conductivity was measured on several samples and averaged at: $K = 0.0122 \text{ cal/sec cm } ^\circ\text{C}$.

The saturation magnetization was measured as a function of temperature with results as shown in Figure 4-6. The extrapolated curie temperature seems to be in excess of 400°C.

The magnetic loss tangent, μ'' , was measured at S-band and as a function of field. The results are shown in Figure 4-7.

To complete the evaluation of this ferrite, the linewidth ΔH is being measured as a function of temperature to fully evaluate the actual operation when the material is used in a hot test.

Several slabs of this material will be evaluated at L-band in the cold test vehicle.

- a. With an aspect ratio $b/a = 4.44 = (0.400 \text{ inch} \times 0.090 \text{ inch} \times 12.0 \text{ inch})$. The applied magnetic field will be adjusted for resonance at $f_r = 1500 \text{ MHz}$ and the band width measured. $H_a \approx 325 \text{ g}$ should be obtained.
- b. With an aspect ratio of 1.250 ($0.156 \text{ inch} \times 0.125 \text{ inch} \times 12.0 \text{ inches}$). The resonance should be obtained at 1500 MHz with an applied field of $H_a = 540 \text{ g}$.

4.2 Broadening techniques. The resonance isolators to be built in the tubes have to cover at least the frequency range of the amplifier considered. In the present case, this is an octave.

Several possibilities are offered.

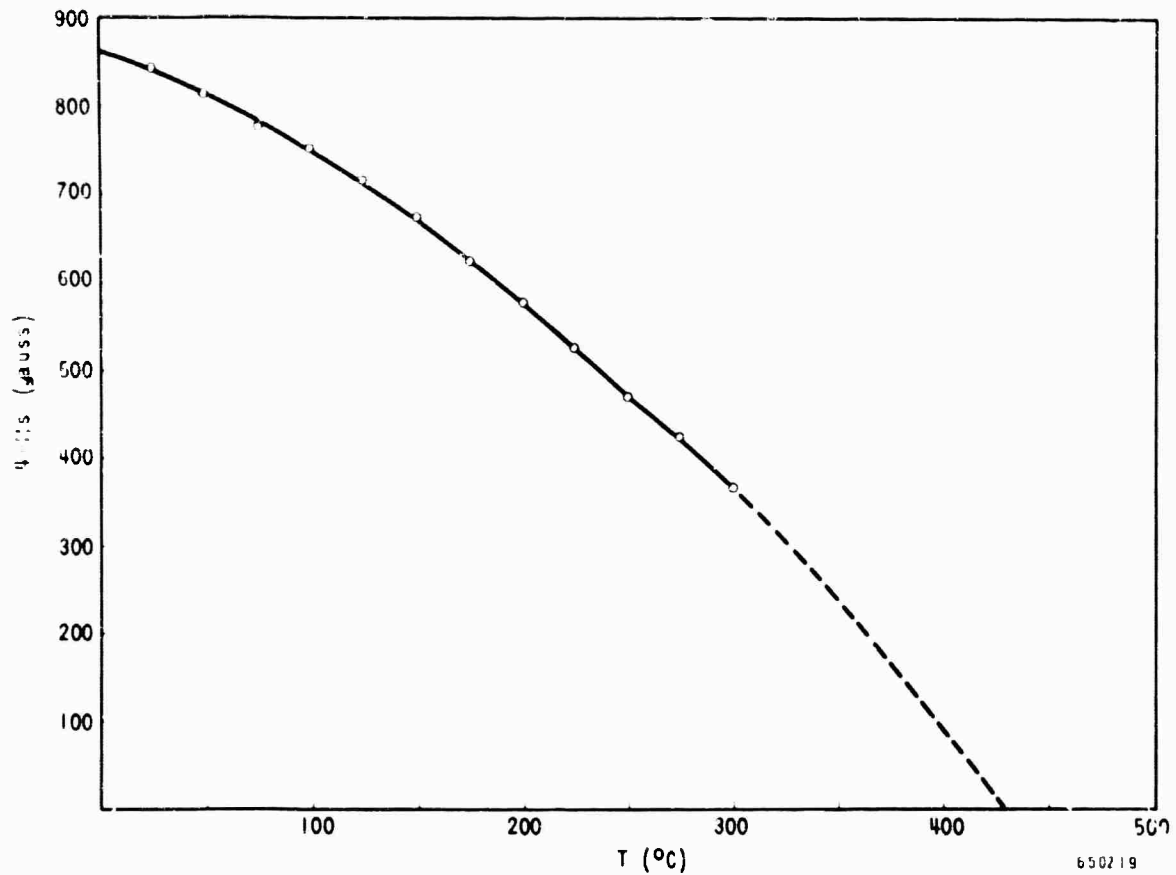


Figure 4-6 Sperry Microwave Electronics Co. Material #40
 $4\pi M_s$ vs Temperature

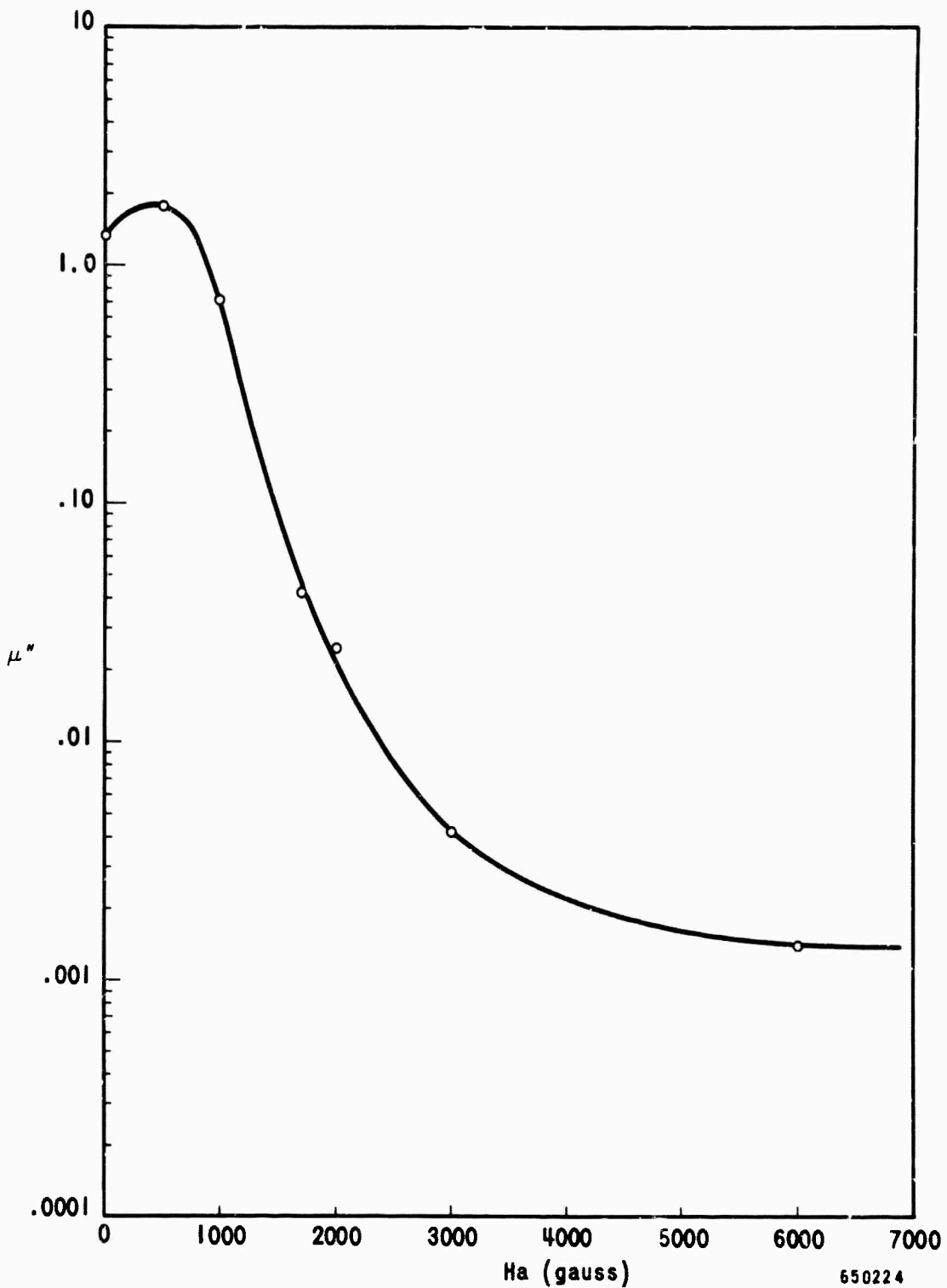


FIGURE 4-7 Sperry Microwave Electronics Material #40
 μ'' vs Applied Magnetic Field (Measured at S-Band)

4.2.1 Using a broad linewidth material.

$$\Delta\omega = \frac{2}{T} = \gamma \Delta H \quad (4-1)$$

relates the bandwidth of the absorption curve (at half power points) with the linewidth of the material.

If a large isolation bandwidth is required, it is then necessary to use a material possessing a large linewidth, but, since the figure of merit is given by

$$R = (\omega T)^2 = \left(\frac{4 w}{\gamma \Delta H}\right)^2, \quad (4-2)$$

the expected back-to-front loss ratio will be relatively small. In the case of an octave bandwidth, it is limited to $R = 36$.

This means that for a given isolation it will be necessary to accept a high insertion loss. At the present time, this property is not thought to be necessarily detrimental to the operation of a crossed-field amplifier, but other considerations such as heating effects may rule it out.

4.2.2 Using a staggered construction.

To increase the figure of merit, it is usual to select a ferrite material with a narrower linewidth. In this case, the frequency range is also narrow.

It is conceivable, in order to increase the operating bandwidth, to use more than one isolator, each incorporating narrow linewidth material but with different resonant frequencies chosen in the band of interest.

The dissipative part of the effective susceptibility can be written for a material subjected to a circularly polarized microwave field as

$$\mu'' \pm = \frac{\omega_{MT}}{(\omega_0 \mp \omega)^2 T^2 + 1} \quad (4-3)$$

where $\omega_M = \gamma 4\pi M_s$
 $\omega_0 = \gamma H_0$ where H_0 is the field at resonance.
 $\omega = \gamma H$
 $T = 2/\gamma \Delta H$ is the relaxation time of the material.

So at resonances where $\omega_0 = \omega$ we have

$$\mu''_+ = \text{reverse loss factor} = \omega_M / T \quad (4-4)$$

$$\mu'' = \text{forward loss factor} = \frac{\omega_{MT}}{(2\omega_0)^2 T^2 + 1} \quad (4-5)$$

Since in most applications

$$2\omega_0^2 T^2 \gg 1 \quad (4-6)$$

we obtain

$$\mu'' = \frac{\omega_M}{(2\omega_0)^2 T} = \frac{\omega_M}{(2\omega_0)^2} \cdot \frac{\gamma \Delta H}{2} \quad (4-7)$$

μ'' will increase with ΔH .

Let us suppose now that we have two ferrite slabs with the same ω_M and T but different ω_0 .

For simplification consider two different slabs of the same volume with resonances at ω_0 and $\omega_0 + \delta$. We can write:

$$\mu'' = \frac{V_1}{V_1 + V_2} \frac{\omega_{MT}}{(\omega_0 + \omega)^2 T^2 + 1} + \frac{V_2}{V_1 + V_2} \frac{\omega_{HT}}{(\omega_0 + \delta + \omega)^2 T^2 + 1} \quad (4-8)$$

where V_1 and V_2 are the volumes of the two ferrites.

Then

$$\mu'' = \frac{\omega_m}{(\omega_0 + \omega)^2 T} \cdot \frac{1}{2} \left[1 + \frac{(\omega_0 + \omega)^2}{(\omega_0 + \delta + \omega)^2} \right]. \quad (4-9)$$

If δ is small compared to $\omega_0 + \omega$, this expression reduces to

$$\mu'' = \frac{\omega_M}{(\omega_0 + \omega)^2 T} \quad (4-10)$$

which is the same as equation (4-6).

In other words, the forward loss will be essentially the one encountered with the narrow linewidth material, but the reverse loss will be spread over a broader range with two peaks at

$$\omega_0 = \omega \quad \text{and} \quad \omega_0 + \delta = \omega$$

Similar results can be obtained by using ferrite with different ω_M , keeping all other parameters the same.

It is then possible to broadband an isolator to some extent without increasing the insertion loss appreciably by:

- a. Changing the demagnetizing factors of slabs made of the same material, subjected to the same applied field.

The difficulty here resides in the fact that the different pieces interact and calculation of the demagnetization factor is almost impossible. Therefore, a solution has to be found experimentally.

- b. Changing the field applied to slabs of a given material with the same demagnetizing factors.

This is impossible in this case because the field applied to the isolator is also the one used by the tube.

- c. Using slabs of different materials having the same demagnetizing factors, subjected to the same applied field.

4.2.3 Using porous ferrite. This case is the same as (a) discussed above. Here the different grains in the ferrite act as resonating domains with different demagnetization factors. Apparent broadening factors of the order of 10 can be obtained without insurmountable problems by increasing the porosity of narrow linewidth materials.

However, such a process will affect other factors, such as thermal conductivity, which might seriously limit the effectiveness of this technique. Eventually, it is probable that a combination of two or more of the methods will be used to meet the tube requirements.

4.3 Use of narrow linewidth material. During this last quarter a possible application of ferrite material to an Amplitron appeared. The tube (discussed previously) was built to operate in the band 2900 - 3100 MHz, but, during test, spurious oscillations were observed in the vicinity of 2850 MHz. It was reasoned that a slab of ferrite absorbing the power at the oscillating frequency would make the tube stable. Since the oscillating frequency was very close to the band-edge, the use of a narrow linewidth material was necessary. The choice, therefore, was to use an yttrium-ion garnet, Raytheon material R171, which has the following measured properties:

$$\begin{aligned} 4\pi M_s &= 1750 \text{ g} \\ \Delta H &= 61 \text{ oe} \\ T_c &= 280^\circ \text{C} \end{aligned}$$

R171 is the only material presently available with the narrow linewidth and high curie temperature. The field applied is the same as the one used by the tube, i. e. $H_a = 2400$ g. To fit the tube, the ferrite must be ring-shaped, and simplified demagnetization factor calculations have shown that an appropriate size would be

1.600 inches OD x 1.130 inches ID x 0.020 inch thick

The ring was tested, but some difficulties were present because of inhomogeneities in the applied magnetic field caused by the conical shape of the pole pieces.

After removing some of the difficulties, it was found that the ring resonated for $H_a = 1950$ g measured at the center of the tube interaction space.

The discrepancy between the observed and the calculated values stems from two sources.

- a. The calculation of the demagnetization factors is only approximate.
- b. The value of the magnetic field in the region occupied by the ferrite is substantially higher than at the center of the tube.

To increase further the resonant field, the shape of the ring was changed to:

1.700 inches OD x 0.900 inch ID x 0.020 inch thick

5. FERRITE MATERIALS RESEARCH

Cold testing to date, using available ferrite materials, has shown that considerably broader line widths will be needed to give the desired octave bandwidth frequency coverage. As an approach toward wide bandwidth without a large change of forward loss, a porous magnesium ferrite was made up and checked for linewidth. As shown by Figure 5-1, a linewidth of 1170 oersteds was achieved under the following conditions:

Material: Magnesium ferrite
 $4\pi M_s = 710$ gauss
Density ~ 70% of theoretical density
 $f_r = 9.2$ GHz

The broad linewidth achieved can be expected to give wide bandwidth with lower forward losses than would have been realized with a 100% density body. The reasoning behind this was indicated in section 4.2.3.

A linewidth temperature run was made on a polycrystalline YIG, with results as shown in Figure 5-2. The decrease of linewidth is due to porosity and a decrease of anisotropy. The linewidth contribution due to porosity is proportional to the saturation magnetization. A minimum reached just below the curie temperature is followed by a large increase as the ferromagnetic-to-paramagnetic transition is crossed.

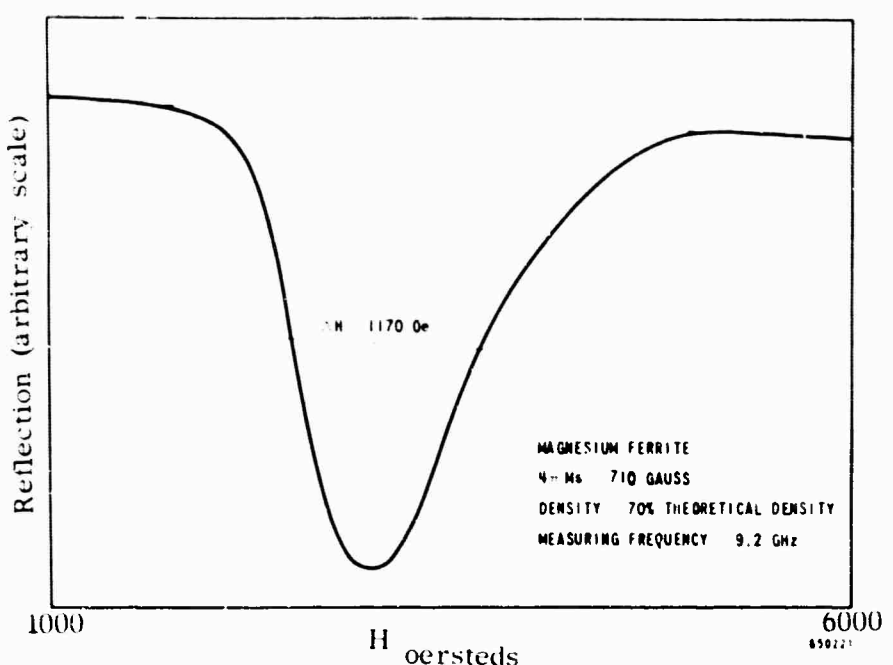


Figure 5-1 Measurement Data for Linewidth of Magnesium Ferrite at X-Band

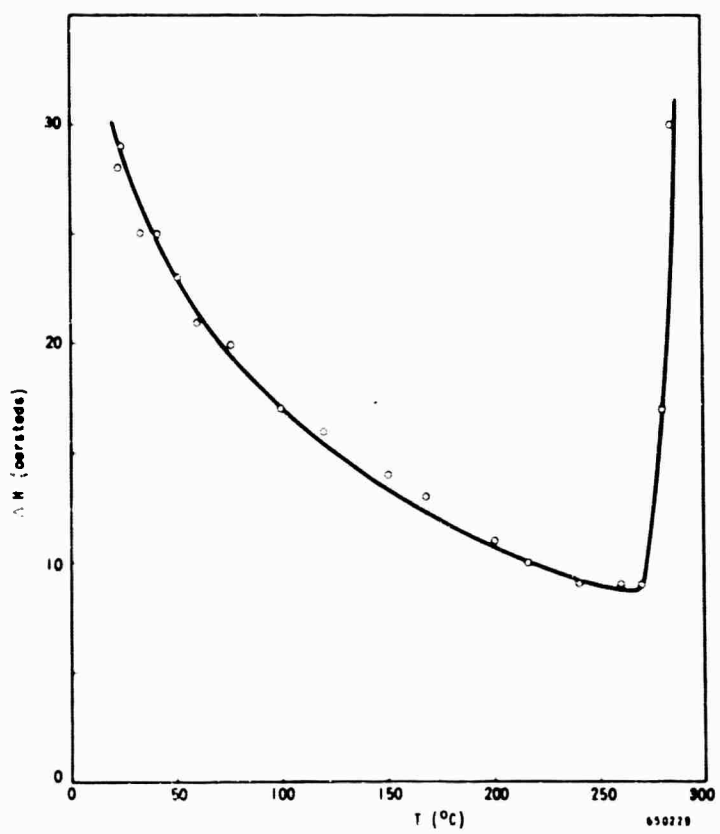


Figure 5-2 Linewidth of Polycrystalline YIG vs Temperature

6. FERRITE BONDING

During this quarterly period, evaluation of ferrite bonds to dielectric materials was continued. Because of a broadened scope of the program, ferrite bonds to metallic substrates are now being prepared. Metallizing of the ferrite is accomplished by sputtering from a heated cathode, and subsequent brazing is carried out in a vacuum furnace.

6.1 Ferrite - ceramic bonds

6.1.1 Mechanical strength. Measurements were performed on ferrite specimens bonded to alumina with soda-lime glass frits as described in the previous report.

<u>Sample No.</u>	<u>PSI in Shear</u>
2-41	2460
2-42	1230
2-43	1135

Examination of samples 2-42 and 2-43 revealed that failure occurred primarily at the bond between the ceramic and the glass frit. Complete "wetting" of this ceramic surface has not taken place. Thus, it seems possible to improve bond strength and assure more uniform bonds by pre-treatment of the ceramic surface with the glass frit material.

6.1.2 Magnetic properties. An additional nickel ferrite sample, glass frit bonded (soda-lime) to alumina in an argon atmosphere, was tested for changes in its magnetic properties.

<u>Sample No.</u>	<u>$4\pi M_s$</u>	<u>Line Width</u>
2-44	319 gauss	416 oersted
R-142 (reference)	453 gauss	303 oersted

6.1.3 Thermal conductivity. Thermal conductivity is being determined in a conventional manner by measuring the surface temperatures and the heat flow through a sample of known geometry under steady state conditions. The rate at which heat is delivered to the sink is found by measuring the temperature rise in the cooling water flowing in the copper base. Since thermocouples are used to measure water temperatures, an increase in precision and resolution was achieved by amplifying the differentially connected thermocouple output with a solid-state operational amplifier. Water flow is determined on a weight/time basis.

Thermal conductivity measurements have been performed on ferrite samples with glass frit bonds using both soda-lime glass and a glass from the system $\text{Na}_2\text{O}-\text{SiO}_2\text{O}_3-\text{Fe}_2\text{O}_3$. These data are not reported because proper interpretation requires measurement of the identical material in the absence of the glass frit bonds. These measurements have not been completed.

6.2 Ferrite to metal bonds.

6.2.1 Preparation of metallized film. Initially, several samples were prepared with an evaporated nickel film, but even with relatively high evaporation rates oxidation of the film occurred when the process was carried out in a vacuum system with the pressure between 10^{-6} and 10^{-5} torr. Electroplating of the resulting metallized film was not possible.

Experiments were next conducted with sputtered nickel films using both cathodic and anodic sources. Best results were obtained when sputtering nickel in argon by using a heated nickel ribbon cathode and an anode-to-cathode potential of approximately 3KV. Although not monitored for film thickness, films prepared by sputtering for one hour as described above were found to have good adherence and were successfully electroplated with additional nickel using conventional plating procedure.

Brazing experiments with the metallized ferrites are now in progress. Preliminary results indicate that ferrite-to-copper bonds using silfos solder are feasible, although a considerable thermal expansion mismatch exists between the two materials.

7.0 CONCLUSIONS

1. Measured forward and backward losses are generally insensitive to the dielectric constant of the support ceramic, but forward losses are slightly greater for the higher of two dielectric constants.
2. An optimum location of the ferrite was determined in the case of the L-band helix model.
3. As expected, no appreciable increase of bandwidth was achieved with higher magnetic fields.
4. Back-to-front ratios obtainable with ferrite mounted on metal are poor, as predicted, but they are not so poor as to preclude their use.
5. Slots in the metal ferrite support have little effect upon the ferrite properties.
6. The feasibility of ferrite mounted in an oil bath has been demonstrated.
7. Ferrite rings, checked for use as bilateral dampers in an S-band Amplitron, have shown promise but at the present time the resonant field is not compatible with the tube field.

8. Broadbanding of ferrites in a CFA can be accomplished by broader linewidths, porous ferrites, and/or staggered construction. It is probable that a combination of these methods will be needed. Measurements made on a porous magnesium ferrite support this conclusion.
9. Bonding of ferrite to dielectric can be effected by the use of glass frit and bonding to copper can be effected by sputtering nickel onto the ferrite in an argon atmosphere and subsequent brazing with silfos solder.

UNCLASSIFIED

Security Classification

DOCUMENT CONTROL DATA - R&D

(Security classification of title, body of abstract and indexing annotation must be entered when the overall report is classified)

1 ORIGINATING ACTIVITY (Corporate author) Raytheon Company, Microwave and Power Tube Division Waltham, Massachusetts		2a REPORT SECURITY CLASSIFICATION Unclassified
		2b GROUP N/A
3 REPORT TITLE RESEARCH ON DISTRIBUTED FERRITES FOR CROSSED-FIELD MICROWAVE DEVICES		
4 DESCRIPTIVE NOTES (Type of report and inclusive date) Quarterly Report #3 - 10 August - 9 November 1966		
5 AUTHOR(S) (Last name, first name, initial) Smith, William A.; Masse, Daniel; Osepchuk, John M.; Plumridge, Robert; Tisdale, Lawrence		
6 REPORT DATE January 1967	7a TOTAL NO OF PAGES 35	7b. NO. OF REFS 0
8a CONTRACT OR GRANT NO. DA28-043-AMC-02032(E)	9a. ORIGINATOR'S REPORT NUMBER(S) PT-1282	
b. PROJECT NO. 7900, 21, 243, 41, 00, 50, 410, 6	9b. OTHER REPORT NO(S) (Any other numbers that may be assigned <i>this report</i>) ECOM 02032-3	
c.		
d.		

10 AVAILABILITY/LIMITATION NOTICES

Distribution of this document is unlimited.

11. SUPPLEMENTARY NOTES SPONSORED BY: Advanced Research Projects Agency - Project Defender Order No. 679 - Amendment No. 1	12. SPONSORING MILITARY ACTIVITY U. S. Army Electronics Command Fort Monmouth, New Jersey 07703 AMSEL-KL-TG
---	--

13 ABSTRACT

The objective of this program is to develop the knowledge and technology necessary to take full advantage of the unidirectional attenuative properties of ferrites in achieving improved gain and bandwidth in crossed-field microwave amplifiers and oscillators. During the third quarterly period, activities included cold testing of ferrite materials in conjunction with an L-band helix, and an investigation of narrow linewidth ferrites in an S-band Amplitron.

Theoretical and Experimental studies have indicated that broadbanding of ferrites in a CFA can be accomplished by broader linewidths, porous ferrites, or by a combination of both methods. Measurements made on a porous magnesium ferrite support this conclusion.

Bonding of ferrites to dielectric can be effected by the use of glass frit, and bonding to copper can be accomplished by sputtering nickel onto the ferrite in an argon atmosphere and subsequently brazing with silfos solder.

UNCLASSIFIED

Security Classification

14 KEY WORDS	LINK A		LINK B		LINK C	
	ROLE	WT	ROLE	WT	ROLE	WT
Ferrites Crossed-Field Amplifiers Delay Line Helix Meanderline Dielectric Loading Split-Folded Waveguide Forward Wave Backward Wave Cw High Power						

INSTRUCTIONS

1. ORIGINATING ACTIVITY: Enter the name and address of the contractor, subcontractor, grantee, Department of Defense activity or other organization (corporate author) issuing the report.

2a. REPORT SECURITY CLASSIFICATION: Enter the overall security classification of the report. Indicate whether "Restricted Data" is included. Marking is to be in accordance with appropriate security regulations.

2b. GROUP: Automatic downgrading is specified in DoD Directive 5200.10 and Armed Forces Industrial Manual. Enter the group number. Also, when applicable, show that optional markings have been used for Group 3 and Group 4 as authorized.

3. REPORT TITLE: Enter the complete report title in all capital letters. Titles in all cases should be unclassified. If a meaningful title cannot be selected without classification, show title classification in all capitals in parentheses immediately following the title.

4. DESCRIPTIVE NOTES: If appropriate, enter the type of report, e.g., interim, progress, summary, annual, or final. Give the inclusive dates when a specific reporting period is covered.

5. AUTHOR(S): Enter the name(s) of author(s) as shown on or in the report. Enter last name, first name, middle initial. If military, show rank and branch of service. The name of the principal author is an absolute minimum requirement.

6. REPORT DATE: Enter the date of the report as day, month, year, or month, year. If more than one date appears on the report, use date of publication.

7a. TOTAL NUMBER OF PAGES: The total page count should follow normal pagination procedures, i.e., enter the number of pages containing information.

7b. NUMBER OF REFERENCES: Enter the total number of references cited in the report.

8a. CONTRACT OR GRANT NUMBER: If appropriate, enter the applicable number of the contract or grant under which the report was written.

8b, &c, & 8d. PROJECT NUMBER: Enter the appropriate military department identification, such as project number, subproject number, system numbers, task number, etc.

9a. ORIGINATOR'S REPORT NUMBER(S): Enter the official report number by which the document will be identified and controlled by the originating activity. This number must be unique to this report.

9b. OTHER REPORT NUMBER(S): If the report has been assigned any other report numbers (either by the originator or by the sponsor), also enter this number(s).

10. AVAILABILITY/LIMITATION NOTICES: Enter any limitations on further dissemination of the report, other than those

imposed by security classification, using standard statements such as:

- (1) "Qualified requesters may obtain copies of this report from DDC."
- (2) "Foreign announcement and dissemination of this report by DDC is not authorized."
- (3) "U. S. Government agencies may obtain copies of this report directly from DDC. Other qualified DDC users shall request through _____."
- (4) "U. S. military agencies may obtain copies of this report directly from DDC. Other qualified users shall request through _____."
- (5) "All distribution of this report is controlled. Qualified DDC users shall request through _____."

If the report has been furnished to the Office of Technical Services, Department of Commerce, for sale to the public, indicate this fact and enter the price, if known.

11. SUPPLEMENTARY NOTES: Use for additional explanatory notes.

12. SPONSORING MILITARY ACTIVITY: Enter the name of the departmental project office or laboratory sponsoring (paying for) the research and development. Include address.

13. ABSTRACT: Enter an abstract giving a brief and factual summary of the document indicative of the report, even though it may also appear elsewhere in the body of the technical report. If additional space is required, a continuation sheet shall be attached.

It is highly desirable that the abstract of classified reports be unclassified. Each paragraph of the abstract shall end with an indication of the military security classification of the information in the paragraph, represented as (TS), (S), (C), or (U).

There is no limitation on the length of the abstract. However, the suggested length is from 150 to 225 words.

14. KEY WORDS: Key words are technically meaningful terms or short phrases that characterize a report and may be used as index entries for cataloging the report. Key words must be selected so that no security classification is required. Identifiers, such as equipment model designation, trade name, military project code name, geographic location, may be used as key words but will be followed by an indication of technical context. The assignment of links, rules, and weights is optional.

UNCLASSIFIED

Security Classification